Discovery of Subnanomolar Arginine-Glycine-Aspartate-Based $\alpha_V\beta_3/\alpha_V\beta_5$ Integrin Binders Embedding 4-Aminoproline Residues

Franca Zanardi,*[,‡] Paola Burreddu,[†] Gloria Rassu,[†] Luciana Auzzas,[†] Lucia Battistini,[‡] Claudio Curti,[‡] Andrea Sartori,[‡] Giuseppe Nicastro,*[,#,||] Gloria Menchi,[§] Nicoletta Cini,[§,○] Anna Bottonocetti,[○] Silvia Raspanti,[○] and Giovanni Casiraghi*[,‡]

Dipartimento Farmaceutico, Università di Parma, Viale G. P. Usberti 27A, I-43100 Parma, Italy, Istituto di Chimica Biomolecolare del CNR, Traversa La Crucca 3, I-07040 Li Punti, Sassari, Italy, Centro Interdipartimentale Misure "G. Casnati", Università di Parma, Viale G. P. Usberti 23A, I-43100 Parma, Italy, Dipartimento di Chimica Organica "Ugo Schiff", Università degli Studi di Firenze, Polo Scientifico e Tecnologico, Via della Lastruccia 13, I-50019 Sesto Fiorentino, Italy, and Dipartimento di Fisiopatologia Clinica, Unità di Medicina Nucleare, Università degli Studi di Firenze, Viale Pieraccini 6, I-50134 Firenze, Italy

Received September 26, 2007

The embodiment of 4-aminoproline residues (Amp) into the arginine-glycine-aspartate (RGD) sequence led to the discovery of a novel class of high-affinity $\alpha_V\beta_3/\alpha_V\beta_5$ integrin binders [$IC_{50h}(\alpha_V\beta_3)$ 0.03–5.12 nM; $IC_{50h}(\alpha_V\beta_5)$ 0.88–154 nM]. A total of eight cyclopeptides of type *cyclo*-[-Arg-Gly-Asp-Amp-], **5**−**12**, were assembled by a standard solid-phase peptide synthesis protocol that involved the C2-carboxyl and C4-amino functionalities of the proline scaffolds, leaving the N^{α}-nuclear site untouched. Functionalization of this vacant proline site with either alkyl or acyl substituents proved feasible, with significant benefit to the integrin binding capabilities of the ligands. Notably, six out of eight cyclopeptide inhibitors, **5**−**7** and **9**−**11**, showed moderate yet significant selectivity toward the $\alpha_V\beta_3$ receptor. The three-dimensional structure in water was determined by NMR techniques and molecular dynamics calculations. Docking studies to the X-ray crystal structure of the extracellular segment of integrin $\alpha_V\beta_3$ complexed with reference compound **1** were also performed on selected analogues to highlight the structural features required for potent ligand binding affinity.

Introduction

Integrins are a large family of heterodimeric transmembrane adhesion glycoproteins, which are responsible for a wide spectrum of cell−cell and cell−extracellular matrixes and cell−pathogen interactions. They participate in bidirectional cell signal transduction resulting in cytoskeleton reorganization, regulation of cell proliferation and cell survival, and apoptosis.[1]

A subset of integrins specifically recognize the tripeptide sequence arginine-glycine-aspartate (RGD[a]),[2] and among these, the integrins of the $\alpha_V\beta_3$, $\alpha_V\beta_5$, and $\alpha_5\beta_1$ subfamilies are directly involved in the evolution and diffusion of metastatic tumor cells and angiogenesis.[3] In truth, these receptor types and, in primis, the $\alpha_V\beta_3/\alpha_V\beta_5$ subfamilies are not generally expressed by epithelial cells nor by normal, quiescent endothelial cells, but become greatly overexpressed by activated endothelial cells and, above all, by metastatic tumor cells. The importance of the $\alpha_V\beta_3$ integrins in angiogenesis during tumor growth is demonstrated by the fact that certain antagonist agents have been successfully used in inhibiting development of the vascular network and tumor growth in various experimental models.[4] Furthermore, systemic administration of $\alpha_V\beta_3$ antagonists induces apoptosis in newly formed blood vessels. The $\alpha_V\beta_5$ integrins are also implicated in angiogenesis processes, although they seem to trigger a pathway of signal transmission distinct from that evocated by their $\alpha_V\beta_3$ relatives.[5] This experimental evidence suggests that the use of dual $\alpha_V\beta_3/\alpha_V\beta_5$ antagonists and selective $\alpha_V\beta_3$ binders both represent viable approaches for the inhibition of tumor angiogenesis and growth.[6]

The use of conformationally constrained cyclic peptides or peptidomimetic entities that broadly survey the molecular space around the integrin RGD binding site has been actively pursued for antagonizing angiogenesis and targeting tumors. The impressive research consolidated over the past decade in this important field has led to the discovery and development of monovalent and multivalent RGD ligands of relevance, with high affinity toward specific integrin receptor subtypes.[4b,7] Among these, we hasten to recall low nanomolar affinity $\alpha_V\beta_3/\alpha_V\beta_5$ dual binders such as the cyclic pentapeptide **1** (EMD121974),[7c,8] the bicyclic lactam-containing derivative **2** (ST1646),[7e,9] the cyclic tetrapeptide **3**,[7g] containing a γ-aminocyclopentanecarboxylic acid (Acpca) fragment, as well as the $\alpha_V\beta_3/\alpha_5\beta_1$ antagonist pentapeptide **4**,[7j] embodying a *cis*-β-aminocyclopropanecarboxylic acid unit (Figure 1).

Worthy of note is compound **3**, which belongs to a series of potent tetrapeptide ligands recently introduced by us, where the

* To whom correspondence should be addressed. Tel.: +39-0521-905067 (F.Z.); +39-0521-905080 (G.C.); +44-2088-162629 (G.N.). Fax: +39-0521-905006 (F.Z.); +39-0521-905006 (G.C.); +44-2089-064477 (G.N.). E-mail: franca.zanardi@unipr.it (F.Z.); giovanni.casiraghi@unipr.it (G.C.); gnicast@nimr.mrc.ac.uk. (G.N.).

‡ Dipartimento Farmaceutico.

† Istituto di Chimica Biomolecolare del CNR.

Centro Interdipartimentale Misure "G. Casnati".

|| Present address: Division of Molecular Structure, National Institute for Medical Research, The Ridgeway, NW7 1AA London.

§ Dipartimento di Chimica Organica "Ugo Schiff".

○ Dipartimento di Fisiopatologia Clinica.

[a] Abbreviations: Bn, benzyl; Boc, *tert*-butoxycarbonyl; DCE, 1,2-dichloroethane; DCM, dichloromethane; DEAD, diethyl azodicarboxylate; DIC, diisopropyl carbodiimide; DIEA, diisopropylethylamine; Diphos, 1,2-bis(diphenylphosphino)ethane; DMF, *N*,*N*-dimethylformamide; DPPA, diphenylphosphoryl azide; Fmoc, 9-fluorenylmethoxycarbonyl; Fmoc-Arg[Pmc]-OH, N^{α}-Fmoc-N^{ω}-(2,2,5,7,8-pentamethylchroman-6-sulfonyl)-L-arginine; Fmoc-Asp[*t*-Bu]-OH, *N*-Fmoc-L-aspartic acid 4-*tert*-butyl ester; Fmoc-Gly OH, *N*-Fmoc-glycine; FmocOSu, 9-fluorenylmethyl-*N*-succinimidyl carbonate; HATU, *O*-(7-azabenzotriazol-1-yl)-*N*,*N*,*N*′,*N*′-tetramethyluronium hexafluorophosphate; HFIP, 1,1,1,3,3,3-hexafluoro-2-propanol; HOAt, 1-hydroxy-7-azabenzotriazole; HOBt, 1-hydroxybenzotriazole; NMP, *N*-methyl-2-pyrrolidinone; RGD, arginine-glycine-aspartate; TBTU, *O*-benzotriazol-1-yl-*N*,*N*,*N*′,*N*′-tetramethyluronium tetrafluoroborate; TFA, trifluoroacetic acid; TIS, triisopropylsilane; TNBS, 2,4,6-trinitrobenzenesulfonic acid; cTrt resin, 2-chlorotrityl chloride resin.

10.1021/jm701214z CCC: $40.75
Published on Web 02/28/2008

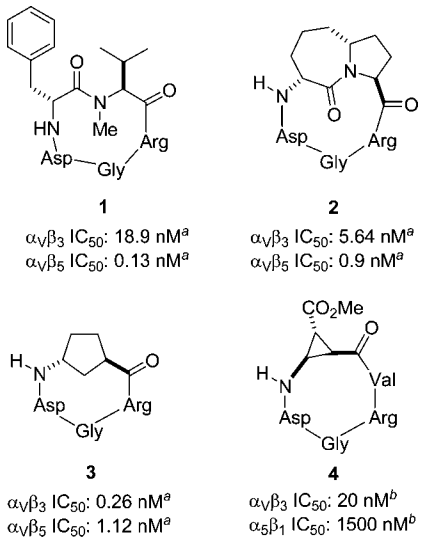

Figure 1. Panel of recently discovered high affinity integrin binders. [a]As determined during the present work; solid phase assay measuring the ability of the cyclopeptide ligand to compete with radiolabeled echistatin in binding to the isolated, immobilized integrin receptor. [b]Ref 7j; cell adhesion assay measuring the ability of the cyclopeptide ligand to inhibit the adhesion of K562 and WM115 cells to vitronectin.

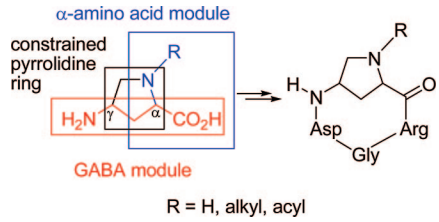

Figure 2. Janus nature of the Amp unit as applied to the synthesis of integrin ligands.

macrocycle backbone encompasses 14 atoms,[10] as opposed to the canonic 15-membered cycles in **1** and **2** or the expanded 16-membered cycle of **4**.

We were delighted to observe that grafting a contracted, conformationally rigid Acpca structure, a sort of α,γ-locked γ-aminobutanoic acid (GABA) surrogate, onto this RGD cycle did, indeed, result in useful conformational arrangements with overall positive outcomes in receptor recognition and binding. We thus wondered whether the insertion of comparably simple, GABA-reminiscent segments into peptide sequences would draw similarly positive results.

The 4-aminoproline nucleus (Amp, 4-aminopyrrolidine-2-carboxylic acid)[11] emerged as a first-class candidate for this investigation, as it combines the structural features of a α,γ-bridged GABA motif with those of the proline ring itself, resulting in a single, multifaceted molecular entity (Figure 2). The central notion of our program was focused on the use of the γ-amino and carboxyl functions of the Amp ring to generate the macrocyclic RGD peptide, leaving the N^{α}-proline site untouched and free for covalent bonding to useful and diverse chemical tethers and functional units.[12] Furthermore, the Amp nucleus presented the added asset of being easily accessible from either commercial sources or by simple chemistry in diverse stereochemical arrangements (D/L, *cis*/*trans*) and substitutions.

In this account we describe the synthesis of a new family of cyclotetrapeptides of type *cyclo*-[-RGD-Amp-], namely, N^{α}-H compounds **5**−**8**, N^{α}-alkyl derivative **9**, and N^{α}-acyl congeners **10**−**12** (Figure 3), and their evaluation as $\alpha_V\beta_3$ and $\alpha_V\beta_5$ integrin competitive antagonists. An in-depth structural analysis was conducted via in-solution NMR measurements, structure calculations, and docking simulations to elucidate the structural features of the new compounds and to rationalize their diverse biological responses.

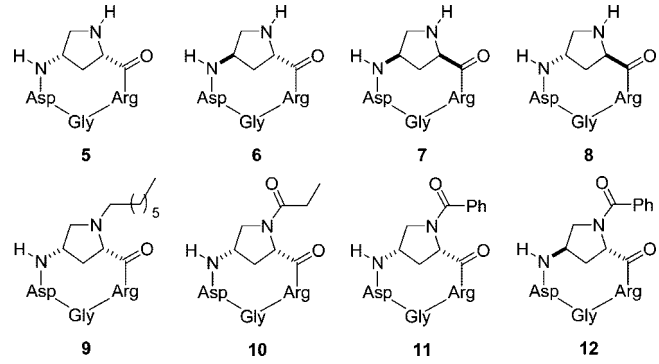

Figure 3. Chemical structures of the eight RGD cyclopeptides in this work.

Scheme 1. Unified Synthesis of 4-Aminoproline Modules **21**−**28**[a]

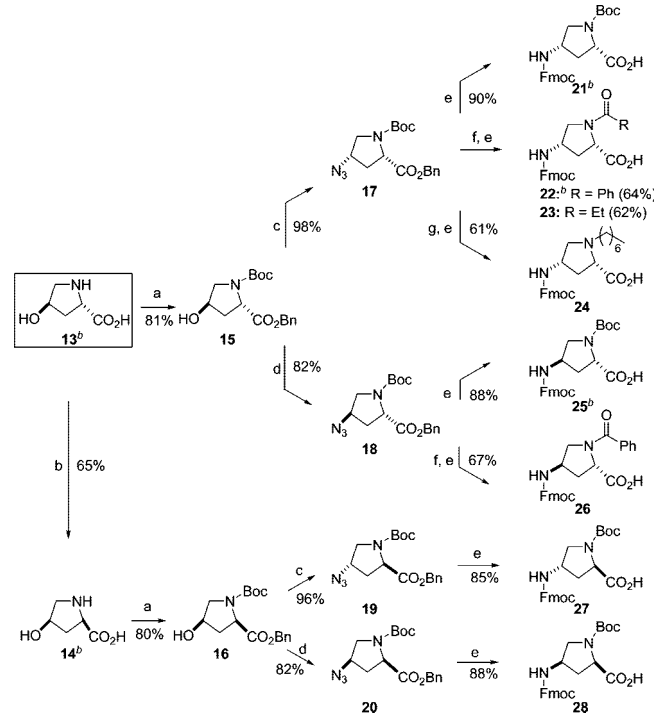

[a] Reagents and conditions: (a) (i) Boc_2O, Et_3N, MeOH, reflux; (ii) Cs_2CO_3, BnBr, MeOH; (b) (i) Ac_2O, AcOH; (ii) 2 N HCl; (iii) Ag_2CO_3; (c) DPPA, PPh_3, DEAD, THF; (d) (i) CBr_4, Diphos, THF; (ii) NaN_3, DMF, 55°C; (e) (i) H_2, Pd/C, MeOH; (ii) FmocOSu, aq Na_2CO_3, THF; (f) (i) TFA, DCM; (ii) benzoic acid (for **22** and **26**) or propanoic acid (for **23**), DIC, HOBt, DCM; (g) (i) TFA, DCM; (ii) heptanal, $NaBH(OAc)_3$, DCE. [b] Commercially available. For details, see the *Supporting Information*.

Results and Discussion

Chemistry. The synthesis program initiated with the in-solution generation of the 4-aminoproline units **21**−**28**, bearing a temporary Fmoc-protection at the N^{γ}-site, as well as a semipermanent Boc-protection at the N^{α}-function (compounds **21**, **25**, **27**, and **28**) or a permanent alkyl/acyl N^{α}-side chain (compounds **22**, **23**, **24**, and **26**). Scheme 1 outlines the divergent synthesis of compounds **21**−**28**, all ultimately arising from the common, commercially available precursor *trans*-4-hydroxy-L-proline (**13**).[13]

Table 1. Inhibition of [^{125}I]-Echistatin Binding to Purified Human Integrin Proteins $\alpha_V\beta_3$ and $\alpha_V\beta_5$ by Compounds **5**–**12**

		one-site model		two-site model			
receptor	cmpd	IC_{50}[a]	Hill slope	IC_{50h}[a]	$\%_h$	IC_{50l}[a]	$\%_l$
$\alpha_V\beta_3$	**5**	4.4 ± 1.0	−0.54	0.47 ± 0.20	45.1	23.7 ± 4.5	54.9
	6	7.01 ± 0.90	−0.77	5.12 ± 0.80	84.5	550 ± 340	15.5
	7	75.14[b]		0.18 ± 0.07	32.3	1350 ± 270	67.7
	8	530 ± 100	−0.61	1.1 ± 1.2	18.0	840 ± 160	82.0
	9	2.84[b]		0.08 ± 0.02	53.7	178 ± 39	46.3
	10	5.60[b]		0.03 ± 0.01	42.1	251 ± 46	57.9
	11	5.15[b]		0.16 ± 0.03	57.8	600 ± 130	42.2
	12	174 ± 39	−0.50	0.91 ± 0.40	31.6	327 ± 47	68.4
	1	18.9 ± 3.1[c]					
	2	5.64 ± 0.40[d]					
	3	0.26 ± 0.06[e]					
	echistatin	0.28 ± 0.08					
$\alpha_V\beta_5$	**5**	80.2 ± 7.4	−0.69	30 ± 11	60.7	390 ± 220	39.3
	6	22.8 ± 2.4	−0.63	1.87 ± 0.37	36.3	53.7 ± 5.0	63.7
	7	154 ± 10	−0.82				
	8	128 ± 16	−1.05				
	9	36.1 ± 3.7	−0.67	0.88 ± 0.23	29.0	62.3 ± 4.3	71.0
	10	94 ± 13	−1.10				
	11	86.6 ± 5.7	−0.96				
	12	89.2 ± 5.4	−0.92				
	1	0.130 ± 0.009[c]					
	2	0.90 ± 0.10[d]					
	3	1.12 ± 0.20[e]					
	echistatin	0.29 ± 0.02					

[a] IC_{50} values (expressed in nM) represent the mean ± SEM of three experiments performed in triplicate. IC_{50h} and IC_{50l} correspond to IC_{50} in the receptor high- and low-affinity states, respectively; $\%_h$ and $\%_l$ represent the proportions of high- and low-affinity states of the receptor. [b] Averaged value estimated by extrapolation of the two-site model values, see ref 25). [c] As determined in the present assay. For literature values, see refs 7c and 7n. [d] As determined in the present assay. For literature values, see refs 7e and 9. [e] As determined in the present assay. For literature values, see ref 7g.

Thus, orthogonal protection of both the secondary amine and carboxyl functions within **13** or its C2-epimer **14**, easily prepared from **13**,[14] gave the corresponding prolines **15** and **16** (81 and 80% yields), whose C4 absolute configuration could be either reverted to the respective azides **17** and **19** (DPPA, PPh_3, DEAD) or retained (doubly reverted) to the corresponding azides **18** and **20** (CBr_4, Diphos; then NaN_3). Stereochemically varied azides **17**−**20** could be converted in parallel to the respective N^{α}-Boc-N^{γ}-Fmoc scaffolds **21**, **25**, **27**, and **28** via catalytic hydrogenation, which concomitantly triggered azide-to-amine reduction and debenzylation, followed by Fmoc carbamoylation (85–90% range yields, two steps).

Addressing the N^{α}-acyl-substituted Amp-modules **22**, **23**, and **26**, L-series azides **17** and **18** were deprotected at the secondary amine site (TFA) and treated with benzoic acid (for **22** and **26**) or propanoic acid (for **23**) in the presence of the activating/condensing DIC/HOBt reagent couple. Subsequent hydrogenolysis and N^{γ}-Fmoc derivatization provided compounds **22**, **23**, and **26** in 64, 62, and 67% yields, respectively, over four steps. As for the heptyl candidate **24**, the alkyl appendage was attached via reductive amination of *N*-deprotected azide from **17** [heptanal, $NaBH(OAc)_3$], followed by usual carboxylic acid and N^{γ}-Fmoc predisposition (61% yield from **17**). Overall, the targeted aminoproline modules were obtained in yields ranging from 38 to 71% from the common precursor **13**.

The next step in the synthesis was the preparation of eight linear protected tetrapeptide precursors of type H-Asp(*t*-Bu)-Amp-Arg(Pmc)-Gly-OH using standard Fmoc-SPPS (solid phase peptide synthesis) chemistry with acid-labile *o*-chlorotrityl chloride resin. The protecting groups of the amino acid side chains were *tert*-butyl (*t*-Bu) for aspartic acid and 2,2,5,7,8-pentamethylchroman-6-sulfonyl (Pmc) for arginine. Briefly, amino acids were coupled stepwise in the presence of TBTU and HOBt coupling reagents. The Fmoc cleavage on the resin was easily performed by the well-established piperidine/DMF procedure. The resin-bound tetrapeptides containing *N*-Boc-protected aminoproline nuclei were cleaved by the mild HFIP/DCM system to avoid premature *N*-deprotection, whereas the remaining linear tetrapeptides were detached from the resin using the usual AcOH/TFE/DCM system. The crude linear peptides were obtained in yields ranging from 35 to 47% for the entire solid phase sequence. Cyclization was achieved at moderate dilution in DMF (3.5 mM) with the HATU/HOAt coupling reagents.

Finally, side-chain deprotection was carried out under acidic conditions (TFA/TIS/water 95: 2.5: 2.5) affording cyclopeptides *cyclo*-[-Arg-Gly-Asp-Amp-], **5**−**12**, with global yields ranging from 57 to 80% for the cyclization/deprotection step. Target compounds **5**−**12** were purified to ≥98% homogeneity by semipreparative reverse-phase HPLC and validated by high-resolution ESI mass spectrometry as well as various NMR techniques (see infra).

Biology. The ability of compounds **5**−**12** to compete with [^{125}I]-radiolabeled echistatin, a viper-derived 49-amino acid disintegrin,[15] in binding to the isolated and purified $\alpha_V\beta_3$ and $\alpha_V\beta_5$ integrins of human placenta[16,17] was evaluated in solid-phase receptor assays[18] and compared with that of known synthetic integrin antagonists **1**,[7c] **2**,[7e,9] and **3**.[7g]

Competition studies were carried out using a fixed concentration of the radioligand (0.05 nM and 0.1 nM for $\alpha_V\beta_3$ and $\alpha_V\beta_5$ receptors, respectively) and a range of concentrations between 100 μM and 0.01 nM of tested molecules. The IC_{50} ± SEM values (nM) were calculated as the concentration of compound required for 50% inhibition of radioligand binding, as estimated by the GraphPad Prism program, with the results reported in Table 1.

Inhibition curves of [^{125}I]-echistatin specific binding were initially fitted to a single-site model equation; however, for most candidates, Hill coefficients significantly differed from unity (e.g., compounds **5**, **6**, **8**, and **12** against $\alpha_V\beta_3$; compounds **5**, **6**, and **9** against $\alpha_V\beta_5$). Moreover, in some cases (compounds **7**, **9**, **10**, and **11** against $\alpha_V\beta_3$), it was not even possible to obtain a concentration–response curve according to the one-site model, due to inconsistent data point fitting. Therefore, the analysis of

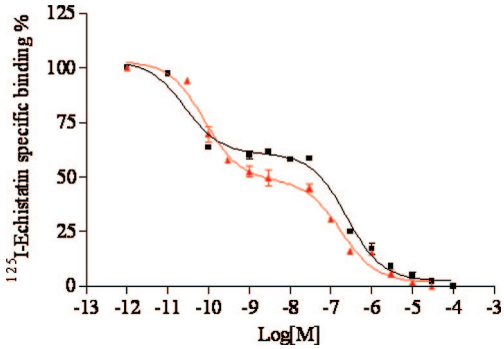

Figure 4. Inhibition of [^{125}I]-echistatin specific binding to purified human integrin protein $\alpha_V\beta_3$ by compounds **9** (red) and **10** (black). Each point represents the mean value ± SEM of triplicate determinations.

the data with nonlinear fitting was better conducted using a two-site model, allowing us to determine IC_{50} values for the high (IC_{50h}) and low (IC_{50l}) affinity states, along with the percent distribution of each affinity site of the receptors.[19] Representative double sigmoidal curves for compounds **9** and **10** are displayed in Figure 4 (see also Figures S9-S16 in the Supporting Information).

The occurrence of two or multiple affinity states of integrin receptors is amply documented,[20] and several authors have described low molecular weight and macromolecular antagonists capable of discriminating different binding states of the receptors. However, to our knowledge, no small sized antagonists have ever been able to prove the coexistence of two or more affinity states of $\alpha_V\beta_3$ and $\alpha_V\beta_5$ integrin receptors in a direct binding assay. The two functional binding states clearly manifested by most candidates in this study are likely to arise from distinct conformational states of a single binding region of the protein that couple to the ligand with different strengths.[1f,20–22] However, ligand binding to two discrete sites of the receptor cannot be ruled out on the basis of the echistatin displacement assay here employed.[23] Be as it may, further biological experiments are necessary to confirm any of the hypotheses described here.

Inspection of the panel of affinity data to $\alpha_V\beta_3$ and $\alpha_V\beta_5$ receptors compiled in Table 1 and calculated according to one-site and two-site binding models reveals several important structure–activity relationships. The SAR analysis can be roughly carried out by comparing the "mean" affinity data[24] obtained from the one-site binding model, except for compounds **7**, **9**, **10**, and **11**, where the one-site fitting calculation cannot be applied. In these cases, for comparative purposes, an estimate of the average binding values was inferred by extrapolation of the experimental two-site model data.[25]

The inhibition values for compounds **5**−**12** toward both $\alpha_V\beta_3$ and $\alpha_V\beta_5$ receptors first indicate a significant nanomolar activity for all candidates, with a major scattering observed for the $\alpha_V\beta_3$ receptor (IC_{50} $\alpha_V\beta_3$ = 2.84–530 nM; IC_{50} $\alpha_V\beta_5$ = 22.8–154 nM). This calls for us to appreciate the impact of subtle structural variations, brought about by the aminoproline module within the ligands, on biological response. The absolute and relative configuration at the C-2 and C-4 stereocenters in the aminoproline module markedly affects the activity profile of the ligands, as shown by direct comparison of the four N^{α}-unsubstituted congeners **5**−**8**. Indeed, for the $\alpha_V\beta_3$ receptor, L-proline-related compounds **5** and **6** with *S*-configuration at C-2 were 17- and 76-fold more potent than the corresponding D-proline-related diastereoisomers **7** and **8**, with 2,4-*cis*-configured isomers **5** and **7** being superior (1.6–5.3-fold) than the 2,4-*trans*-counterparts **6** and **8**. The higher activity of the ligands embodying L-series proline **5** and **6** is also conserved for the $\alpha_V\beta_5$ receptor, although this discrepancy is minimal.

It is interesting to note that the most potent representative of the unsubstituted series, compound **5**, with a mean activity for the $\alpha_V\beta_3$ receptor of 4.4 nM (one-site model) displays almost an equal proportion between the high affinity (0.47 nM) and low affinity (23.7 nM) states, while the epimeric ligand **6** manifests two highly differentiated high and low affinity states (5.12 vs 550 nM) in the ratio 85:15 high/low.

The three N^{α}-unsubstituted derivatives **5**−**7** invariably show a significant binding propensity for the $\alpha_V\beta_3$ receptor, with selectivity ratios $\alpha_V\beta_3/\alpha_V\beta_5$ of 18, 3, and 2, respectively; and this trend is recurrent in the other derivatives of the same group, with exception to ligands **8** and **12**, where a reverse in selectivity is observed.

With the low-nanomolar prototype **5** at hand, substitution at the N^{α}-site of the proline nucleus was evaluated, using N^{α}-alkyl and N^{α}-acyl appendages. Replacement of a hydrogen atom with a *n*-heptyl group within compound **9** markedly exalted the binding activity for both receptors, with about a 2-fold enhancement. This potent integrin binder sharply distinguishes two binding sites in both receptors, with picomolar affinity for the high affinity site (IC_{50h} $\alpha_V\beta_3$ = 80 pM, 54% occupancy; IC_{50h} $\alpha_V\beta_5$ = 880 pM, 29% occupancy).

N^{α}-acyl substituted candidates **10** and **11** show a "mean" activity comparable to that of N^{α}-H parent compound **5**, although their potency seems exalted when high-affinity IC_{50} values are considered (0.03 nM and 0.16 nM vs 0.47 nM). Noticeably, while compounds **10** and **11** unequivocally discriminate between two binding states of the $\alpha_V\beta_3$ receptor (double sigmoidal competition curves), these same compounds failed to do so when tested against the $\alpha_V\beta_5$ receptor (single sigmoidal competition curves; see Figures S14 and S15 in the Supporting Information).

Overall, the entire set of biological data suggest that the embodiment of 4-aminoproline modules into the RGD sequence leads to a new class of potent $\alpha_V\beta_3$ and $\alpha_V\beta_5$ integrin binders. Among the proline scaffolds, quickly accessible *cis*-disposed 4-amino-L-proline residues are the best candidates for the construction of ligands with astonishing potency. Furthermore, positioning hydrophobic, relatively mobile alkyl or acyl chains at the N^{α}-site of the proline subunit, as in candidates **9**, **10**, and **11**, greatly improves the activity profile by possibly increasing the receptor recognition capability of the RGD sequence (see infra).

L-Proline-based compound **5** and its relatives **9**, **10**, and **11**, besides being among the best $\alpha_V\beta_3$ integrin antagonists developed so far, with affinity approaching or even surpassing those of standard small-sized ligands **1**, **2**, and **3**, display a singular virtue that, to our knowledge, has never been reported previously in low molecular weight integrin binders during direct binding assays; that is, the ability to demonstrate, beyond any doubt, the occurrence of two affinity states in the $\alpha_V\beta_3$ and $\alpha_V\beta_5$ integrins.

Whether this fact is interpreted as evidence for the existence of alternative conformations of the single receptor when in the active ligand-bound state, or whether it suggests ligand binding to two discrete sites on the receptor, active compounds such as **5**, **9**, **10**, and **11** may represent remarkable biological and pharmacological tools for in-depth study of the structural and functional features of integrin machinery.

NMR Spectroscopy and Solution Structural Analysis. The complete chemical shift assignment of proton and carbon

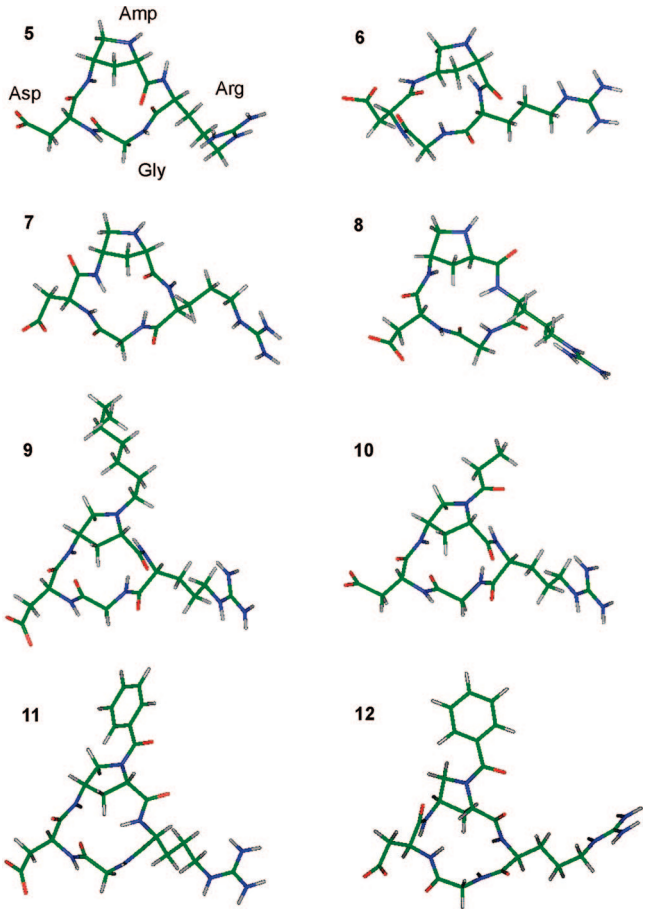

Figure 5. NMR-derived minimum energy conformations of analogues **5**−**12**. Highly active compounds **5**, **9**, **10**, and **11** have a strong tendency to adopt stabilizing inverse γ-turns centered at the Asp residue, forming a hydrogen bond between AmpNH and GlyCO. Conversely, less-active compounds **8** and **12** lack defined structural motives, resulting in rather flat structures. Color code: green, carbon; gray, hydrogen; blue, nitrogen; red, oxygen.

resonances for cyclopeptides **5**−**12** has been carried out for water solutions (90% H_2O/10% D_2O) using one- and two-dimensional NMR experiments (TOCSY, COSY, ROESY, and NOESY), following the standard procedure described in the Experimental Section.

A qualitative analysis showed that the ^{1}H NMR spectra of compounds **5**−**8** revealed the presence of single species (>95%), whereas for compounds **11** and **12**, the existence of two main forms in a ∼1:1 ratio was evident, which interchange slowly on the NMR time scale. These two forms are clearly ascribed to *trans–cis* isomers at the Cα−N−CO−phenyl dihedral angle. Similarly, compound **10** showed two forms in a 9:1 ratio, recognizable as *trans–cis* isomers at the Cα−N−CO−ethyl bond. As for compound **9**, bearing an heptyl chain at the N^{α}-site of the proline scaffold, a more complicated picture was found, with one main and two minor species in an approximately 8:1:1 ratio. Due to overlap problems, only the spectra of the major form of **9** could be assigned.

All the analogues of this eight-member family of $\alpha_V\beta_3/\alpha_V\beta_5$ binders, compounds **5**−**12**, were analyzed and their NMR three-dimensional solution structures determined (Figure 5). An evaluation of the ROE connectivities in compounds **5**, **7**, **9**, **10**, and **11**, all embodying a 2,4-*cis*-disposed aminoproline subunit, showed the presence of medium-strong sequential $d_{\alpha N(i,i+1)}$ ROEs along the entire peptide sequence with medium-strong $d_{NN(i,i+1)}$ ROEs between Asp-NH and Amp-NH. For the single forms of **5** and **7**, as well as the major forms of **9**, **10**, and **11**, the $^3J_{NH\text{-}\alpha H}$ coupling constant of the Asp residue was ≥9 Hz, which is an indication of stable structures.

As for compounds **6**, **8**, and **12**, bearing a 2,4-*trans*-aminoproline scaffold, detection of only medium intensity $d_{\alpha N(i,i+1)}$ connectivities along the peptide and the presence of $^3J_{NH\text{-}\alpha H}$ coupling constants in the range typical for fast conformational averaging (6.2–7.3 Hz) suggest that **6**, **8**, and **12** are flexible, in equilibrium with multiple conformations.

Further structural information was obtained by studying the temperature dependence of the chemical shifts of NH protons covering the range between −4.0 ppb/K for Amp-NH and −10 ppb/K for Arg and Asp NHs. As an exception, for the Amp-NH of compounds **7** and **11**, temperature coefficients $\Delta\delta/\Delta T$ of −1.1 and −1.6 ppb/K indicated the presence of a stable hydrogen bond.

For these compounds, a total of 100 three-dimensional structures satisfying ROEs and dihedral angle constraints ($^3J_{NH\text{-}\alpha H}$) were generated, using simulated annealing (SA) calculations. The structures with the lowest energies and with no ROEs >0.3 Å violation were selected and clustered in families based on pairwise root-mean-square deviations (rmsd) of the backbone residues. Compounds **5** and **7** could be clustered into a major family corresponding to >80% of the selected structures (the rmsd of the backbone for the structures of the major family were 1.2 and 1.1 Å, respectively), while compounds **10**, **11**, and **12**, whose NMR spectra showed the coexistence of two slowly interchanging *cis–trans* conformational states, are characterized by the existence of a major family in the *trans*-conformation (compound **10**, 90% occurrence) or the existence of a main population both in the *trans* and *cis* forms (compounds **11** and **12**, >80% occurrence). For peptide **10**, an ROE between the H2′ protons of the acyl tail and the H5 within the Amp ring was indicative of a *trans*-conformation, while the same *trans*-arrangement of **11** and **12** was supported by ROE contacts between the aromatic Hδ protons and the H4 and H5 protons of the Amp scaffolds. For compound **9**, comparison of rmsd values of the obtained structures revealed two different families. About 75% of the structures belong to the first family, which includes the lowest energy structure. Because strong ROEs between protons Amp-NH, Asp-Hβ, and Amp-Hγ would be expected from the structures of the least populated families, but such ROEs were nonobservable, this structural family was not considered further.

Overall, the conformational study suggests that cyclotetrapeptides **5**, **7**, **9**, **10**, and **11**, the best $\alpha_V\beta_3$ antagonists in the series, are characterized by the presence of a common motif that can be identified as an inverse γ-turn structure.[26] In particular, from the analysis of the dihedral angles, an inverse γ-turn could be observed around the Gly-Asp-Amp-NH residues (**5**: $<\phi_{i+1}> \sim -110°$, $<\Psi_{i+1}> \sim 70°$; **7**: $<\phi_{i+1}> \sim -80°$, $<\Psi_{i+1}> \sim 75°$; **9**: $<\phi_{i+1}> \sim -80°$, $<\Psi_{i+1}> \sim 80°$; **10**: $<\phi_{i+1}> \sim -90°$, $<\Psi_{i+1}> \sim 60°$; **11**: $<\phi_{i+1}> \sim -100°$, $<\Psi_{i+1}> \sim 60°$). This stable inverse γ-turn conformation was unambiguously supported by strong $d_{NN(i,i+1)}$ ROE contacts between Asp-NH and Amp-NH, the large $^3J_{NH\text{-}\alpha H}$ coupling constant (≥9 Hz) for Asp, as well as the relatively low temperature coefficient of Amp-NH. Specifically, the $\Delta\delta/\Delta T$ values for Amp-NH ranging from –1.6 to –4.0 ppb/K are consistent with a considerable shielding of this proton and its involvement in intramolecular hydrogen bonding.

Tetrapeptides **6** and **8**, on the other hand, do not adopt preferential conformations, as suggested by the aforementioned NMR restraints, indicating that these peptides are flexible, with

diverse conformations rapidly interconverting in solution. Owing to their enhanced flexibility, clusters of conformers could not be obtained with high separation ratios, implying that **6** and **8** fold themselves in multiple ways. In particular, for **6**, inspection of the dihedral angles around the Asp residue reveals that it is possible to group the structures into six main conformations (<Φ>, 60° or –60°; and <Ψ>, 60°, 100°, –60°, –100°), whose populations amount to 90%, while for **8**, this analysis shows that there are two preferential subsets of values for both angles (<Φ>, 60° or –100°; and <Ψ>, 100° or –80°). The large conformational diversity is indicated by the rmsd values calculated for these structures (2.1 Å for **6** and 2.3 Å for **8**). As for peptide **12**, the ROEs assignment was complicated due to the presence of several overlapping resonances, and two sets of NMR spectra were collected at different temperatures (298 and 303 K). The refined ensemble indicated the presence of preferential subsets of backbone values on the Asp residue (<Φ>, ∼75° or –77°; and <Ψ>, –106°), thus suggesting a nonpreferential orientation.

For this subfamily of conformationally unrestricted analogues, especially compounds **8** and **12**, the loss of entropy upon binding is increased compared to a ligand with a definite preorganized structure, and this may be responsible for the significant loss of binding capability.

In all the analyzed compounds of this series, a certain flexibility within the Arg and Asp side chains was found, which causes them to point away from the macrocyclic backbone and exposes them to the solvent.

It is worth pointing out that the critical distance between the Cβ atoms of Arg and Asp residues is kept at 7.8–8.2 Å in all the analyzed structures, except for compound **6**, which displays an extended 8.8 Å distance.

At this point, it would be useful to critically compare the structural and conformational arrangement of the ligands in this study and their integrin binding affinity to the structural and biological data emerged from recent crystallographic and molecular modeling studies performed on the reference candidates **1**, **2**, and **4**, as well as our own first-generation aminocyclopentanecarboxylic acid-containing RGD derivatives of type **3**. Compound **1**, a 15-membered pentapeptide macrocycle, adopts a conformation characterized by an inverse γ-turn with Asp at position ($i + 1$) and a distorted βII′-turn with Gly and Asp at the ($i + 1$) and ($i + 2$) positions, respectively. An 8.9 Å distance between the Arg and Asp Cβ atoms and an extended conformation of the RGD sequence were also observed for this ligand in the solid state.[22b] Compound **2**, again comprising a 15-atom macrocycle, was reported to assume preferred conformations very similar to the X-ray $\alpha_V\beta_3$-bound conformation of **1** (average Cβ(Arg)-Cβ(Asp) 8.5 Å).[9b] The close structural similarity of these two ligands is reflected in a strictly related binding profile, with dual $\alpha_V\beta_3/\alpha_V\beta_5$ affinity values in the low-nanomolar range. On the other hand, 16-membered pentapeptide ligand **4**, carrying a constrained β-aminocyclopropanecarboxylic acid (β-Acc), featured a γ-turn at Gly, along with a pseudo-β turn at β-Acc-Val.[7j] With a mean distance between the Cβ atoms of Arg and Asp of 7.06 Å, ligand **4** exhibited an overall potency of 20 nm against $\alpha_V\beta_3$, suggesting that the $\alpha_V\beta_3$-binding domain may also tolerate more expanded peptide macrocycles, provided that bent RGD sequences are involved.

Our first-generation ligand series, including the best nanomolar dual candidate **3**, all embody an aminocyclopentanecarboxylic acid moiety (Acpca) en lieu of the aminoproline module of the present work. In-solution 3D NMR structural results revealed that the contraction of the macrocycle to a 14-membered ring structure did not compromise development of high affinity binders and that an organized arrangement of the cyclopeptide backbone (an inverse γ-turn motif or an organized kink centered at Asp), along with Cβ Arg-Asp distances in the range 8.0–8.5 Å, proved essential for efficient $\alpha_V\beta_3/\alpha_V\beta_5$ integrin binding.[7g]

Superposition (not shown) of the lowest energy structures determined by in-solution analysis of highly active Amp-RGD compounds **5**, **9**, **10**, and **11** of this study with the minimum energy structures of our first-generation Acpca-RGD representatives revealed an astonishing structural resemblance, especially for the part of the backbone belonging to the inverse γ-turn (average rmsd for the backbone atoms of Arg-Gly-Asp-NH residues in the 0.1–0.5 Å range). This good conformational resemblance, along with the high binding potency displayed by the ligands in both series, collectively suggest that the common inverse γ-turn motif in the region Gly-Asp-Amp-NH (or Gly Asp-Acpca-NH) is highly beneficial for efficient binding to $\alpha_V\beta_3$ and $\alpha_V\beta_5$ integrin receptors.

However, these observations alone do not fully explain the increase in $\alpha_V\beta_3$ activity and $\alpha_V\beta_3/\alpha_V\beta_5$ selectivity of some compounds in the present series as compared to the previously reported candidates. Likely, the presence of the nitrogen atom in the proline scaffold of the Amp-RGD ligands (en lieu of a carbon atom in Acpca-RGD relatives), significantly altered the ratio between the $\alpha_V\beta_3$ and $\alpha_V\beta_5$ binding affinity, while retaining or even improving potency toward the $\alpha_V\beta_3$ receptor (compounds **5**, **9**, **10**, and **11**, IC_{50h} in the picomolar range). Thus, this SAR conclusion suggests that, at least for the most potent compounds in this series, the introduction of the *N*-heteroatom into the ligand's core structure offers the opportunity to gain improved $\alpha_V\beta_3$ binding properties and modest, yet significant $\alpha_V\beta_3$ vs $\alpha_V\beta_5$ selectivities.[27]

Docking Simulation. To gain further insight into the relationship between the activity profile of the aminoproline-containing cyclopeptides in this study and their in-solution structure and to investigate the possible binding modes of these ligands to the $\alpha_V\beta_3$ receptor on a molecular level, a docking simulation was performed, choosing subnanomolar candidates **5**, **9**, and **10**.

The protein binding site was derived from the X-ray crystal structure of the extracellular segment of the $\alpha_V\beta_3$ integrin complexed with the known pentapeptide ligand **1** (Protein Data Bank, entry 1L5G).[22b] It was found that the Asp carboxylate and the Arg guanidinium moiety in ligand **1** are the two structural features crucial for the receptor recognition. In particular, the binding site revealed that two manganese atoms in the metal ion dependent adhesion site (MIDAS) and in the adjacent ADMIDAS region interact with the negatively charged portion of the ligand, while four carboxylate residues, Asp150, Asp218, and Asp219 (on the α_V subunit), and Asp217 (on the β_3 subunit) bind to the positively charged guanidinium group. Furthermore, the Asp group of **1** exhibits interactions with the Tyr122 and Asn215 backbone amides.

The docking program AutoDock 4.0.1[28] was used to evaluate the binding energies of compounds **5**, **9**, and **10** as potential ligands for the $\alpha_V\beta_3$ receptor and the docked structures were compared to the crystal structure of the bound ligand−protein complex. After addition of the hydrogen atoms to the crystal structure 1L5G, the ligand **1** was removed and the protein was charged and prepared for its use in the subsequent docking study, as described in the Experimental Section. The lowest energy docked structures were evaluated for the possible interactions with the ligand binding site of the $\alpha_V\beta_3$ integrin receptor. To

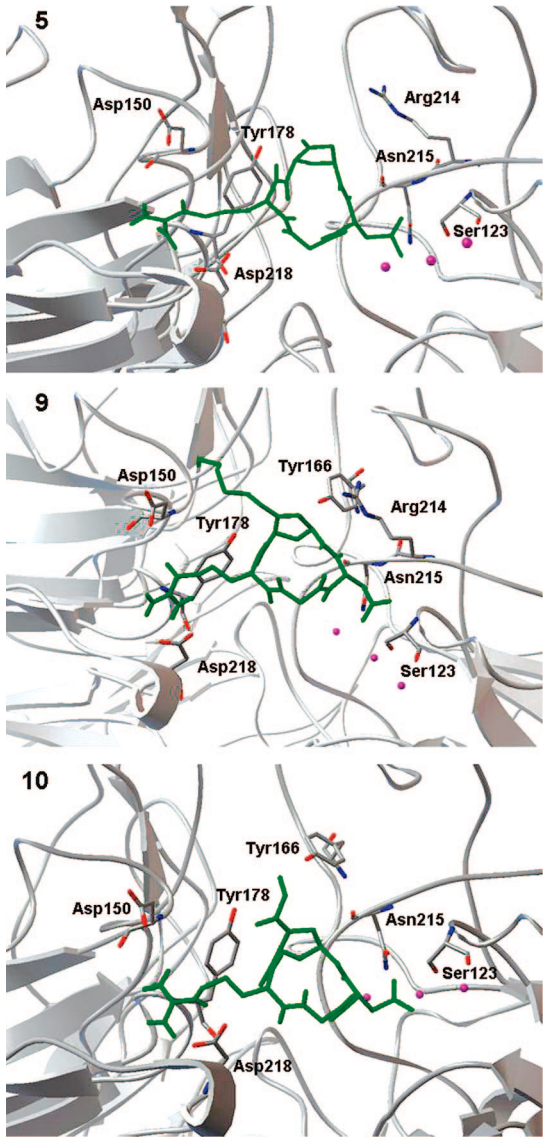

Figure 6. Representation of the RGD ligands **5**, **9**, and **10** docked into the binding region of $\alpha_V\beta_3$ integrin (as reported by J.-P. Xiong et al.[22b]) highlighting the protein residues that form the main interactions with the different structural units of the ligands. For **5**: Asp150 and Asp218 vs Arg; Asn215, Ser123, Arg214, and Mn^{2+} vs Asp; Tyr178 vs Amp-N^{α}-H. For **9**: Asp150 and Asp218 vs Arg; Asn215, Ser123, Arg214, and Mn^{2+} vs Asp; Tyr166 and Tyr178 vs Amp-N^{α}-heptyl. For **10**: Asp150 and Asp218 vs Arg; Asn215, Ser123, and Mn^{2+} vs Asp; Tyr166 and Tyr178 vs Amp-N^{α}-propanoyl. The manganese ions are shown in magenta. Nonpolar hydrogen atoms of the ligands are omitted for clarity.

analyze the binding modes of ligands **5**, **9**, and **10**, we checked the crystal structure of the complex between the $\alpha_V\beta_3$ protein and its reference inhibitor **1**. The superposition of the C^{α} trace of **1** onto analogues **5**, **9**, and **10** in the docked conformations yielded average rmsd values of 0.21, 0.17, and 0.15 Å, respectively. The similar architecture between ligands **5**, **9**, and **10** and **1** allowed us to decipher the possible interactions that peptides **5**, **9**, and **10** could experience within the $\alpha_V\beta_3$ receptor.

We visually checked the top scoring poses for compounds **5**, **9**, and **10** and a common binding mode was identified (Figure 6 and additional Figures S17−S19). The docking experiments indicated that the structures reproduced very closely the crystallographic binding mode displayed by reference compound **1**. In particular, the high-score modes evidence that firm ionic interactions exist between the guanidinium portion of the ligands and the Asp150 and Asp218 residues (α_V portion) and highlight that the aspartic acid side chain fits into a short, narrow pocket that houses a manganese cation and, at the same time, interacts with the backbone amide hydrogen of Asn215 and/or with the Ser123 side chain (β_3 portion). In addition, the network of hydrogen bonds between the ligands and the receptor may involve the backbone CO of Asp with the Arg214 side chain.

Docking of compound **5**, embodying a vacant N^{α}-proline site, revealed a well-clustered assemblage, with 50 runs converging to a small number of different positions (32 similar positions out of 50). Besides the basic interactions involving the Asp and Arg residues (vide supra), a notable H-bonding contact between the free proline NH and Tyr178 hydroxyl was observed, which could possibly stabilize the positioning of the ligand within the binding pocket.

For compounds **9** and **10**, where the N^{α}-site of the proline nucleus is substituted by alkyl or acyl moieties, it was found that these side chain groups point toward a large hydrophobic hollow formed by Tyr178, Trp179, and Phe154 (on α_V) and by Tyr122 and Tyr166 (on β_3), with major binding modes involving a favorable interaction with the Tyr166 and Tyr178 aromatic rings. Furthermore, in the case of **10**, the carbonyl-acyl group is positioned to form a hydrogen bond with Tyr178 hydroxyl and thus helps to stabilize the network of hydrogen bonding. Assuming that the X-ray pose chosen as the model in this study describes an advantageous interaction mode between the ligand and the $\alpha_V\beta_3$ receptor, these findings could explain the substantial increase in binding affinity when passing from the unsubstituted analogue **5** (IC_{50h} 0.47 nM) to *N*-alkyl derivative **9** (IC_{50h} 0.08 nM) and to the *N*-acyl congener **10** (IC_{50h} 0.03 nM).[29]

The backbone rms differences between the docking structures and the NMR solution structures were in the range 1.1–1.5 Å; however, these deviations were also present in the rms of the NMR-derived solution structures of the same compounds. The peptide cores of **5**, **9**, and **10** were largely preserved in the docking models, retaining the inverse γ-turn conformations. The interproton distance restraints derived from experimental ROEs were compared with the docked structures. The structures satisfy the experimental restraints rather well; there are neither distance violations greater than 0.5 Å, nor backbone dihedral angle violations greater than 30°. From these results, it is clear that the mean backbone docking conformations of the analyzed ligands did not change considerably during the docking, remaining close to the mean initial structures. Conversely, modest changes of the side-chain conformations (not farther than 4.5 Å) could be observed.

Summarizing, two major points emerge from this analysis: (1) docking results for each Amp-containing cyclopeptide bound to the $\alpha_V\beta_3$ integrin are substantially consistent with in-solution three-dimensional NMR structural evidence; and (2) the key ligand–receptor interactions, the characteristic Arg-Asp Cβ-distances, the overall peptide backbone arrangement, and the side chain geometry observed in the crystalline complex of **1** with the $\alpha_V\beta_3$ protein appeared to be almost nearly maintained in the top-ranking docked poses of high affinity ligands **5**, **9**, and **10**. A superposition of docked structures **5**, **9**, and **10** to the X-ray $\alpha_V\beta_3$-bound conformation of **1** is reported in the Supporting Information (Figure S19).

Conclusion

The work was founded on the idea that readily available 4-aminoproline could serve as a useful core in the construction of macrocyclic RGD peptides to be used as integrin binders.

This idea was then successfully put into practice. Indeed, covalent incorporation of a series of stereochemically varied 4-aminoproline modules bearing diverse substituents at the N^{α}-site into the RGD sequence led to the discovery of a new class of $\alpha_V\beta_3$ and $\alpha_V\beta_5$ integrin ligands, whose in vitro bioactivity proved to be remarkable.

All the synthesized cyclopeptides, namely, compounds **5**−**12** showed ligand competence in the low nanomolar range for both α_V receptors, with β_3 affinity values reaching outstanding levels, as observed for picomolar lead compounds **9** and **10** [$IC_{50h}(\alpha_V\beta_3)$ 0.08 nM and 0.03 nM, respectively].

Worthy of note is the observation of the double sigmoidal competition curves displayed by most candidates during the [^{125}I]-echistatin-based competition binding assay, which indicates that such ligands are able to discriminate between two affinity states of the targeted integrin receptors. While the in-depth reasons for this behavior are still to be fully explained on a biomolecular level, we consider this a valuable result in view of their possible use in targeted therapies and their potential as molecular probes. In their latter role, these ligands could help unravel the complexities associated with integrin structure and function.

In-solution structural studies and SAR analysis of ligands **5**−**12**, as well as docking simulations performed on three selected compounds, **5**, **9**, and **10**, concurred to reveal that, for the most active candidates in this study, the basic structure adopted by the tetrapeptide backbone is an inverse γ-turn centered at the Asp residue, and this seems to confer the correct conformational arrangement for the most appropriate interaction with the receptor. Furthermore, the N^{α}-alkyl and acyl tails within the proline ring of compounds **9** and **10**, far from being lame bystanders, provide critical subsidiary contacts with the receptor, while modulating the hydrophobic/hydrophilic character of the ligand itself. Clearly, the positioning of lipophilic alkyl or acyl chains in a hydrophobic subpocket, formed mainly by (α_V)-Tyr178, Trp179, Phe154, and (β_3)-Tyr122, Tyr166 residues, is a crucial requirement for enhanced affinity binding.

Thus, while a new family of $\alpha_V\beta_3/\alpha_V\beta_5$ integrin binders has been discovered, with compounds **5**, **9**, and **10** emerging as promising lead candidates, the challenge is to develop promiscuous, multitarget-directed compounds[30] by exploiting the N^{α}-proline anchorage of the RGD ligands and utilize them to tackle the multifactorial nature of cancer and cognate integrin-involving diseases.[31] This is underway.

Experimental Section

General experimental information and details of the synthetic procedures for compounds **15**−**28** are given in the Supporting Information.

***cyclo*-[-Arg-Gly-Asp-Amp21-] (5). General Procedure for Cyclopeptide Synthesis. Solid Phase Synthesis.** The synthesis of the linear tetrapeptide H-Asp(Bu^t)-Amp**21**-Arg(Pmc)-Gly-OH was performed using Fmoc-based solid-phase peptide synthesis with cTrt resin (loading 1.55 mmol/g). *Resin loading*: In a solid phase reaction vessel, to the cTrt resin (178 mg, 0.276 mmol) preswollen in DCM (30 min) a solution of Fmoc-Gly-OH (206 mg, 0.69 mmol) and DIEA (110 μL, 0.635 mmol) in DCM (2.5 mL) was added. The reaction mixture was stirred under a flow of nitrogen for 1 h. After adding another 110 μL of DIEA (0.635 mmol) and 500 μL of MeOH, the mixture was shaken for an additional 30 min and then drained, and the resin was extensively washed with DMF (3 × 3 mL), DCM (5 × 3 mL), *i*-PrOH (2 × 3 mL), MeOH (5 × 3 mL), Et_2O (2 × 3 mL), and DCM (3 × 3 mL). The Fmoc-Gly resin, swollen in DMF (5 × 3 mL), was treated with 5% v/v piperidine in DMF/DCM 1:1 (5 mL, 5 min). The solution was drained and the resin was treated with 20% v/v piperidine in DMF (5 mL × 5 min × 6 cycles). The resin was extensively washed with DMF (3 × 3 mL), *i*-PrOH (3 × 3 mL), Et_2O (3 × 3 mL), DCM (3 × 3 mL), and DMF (2 × 3 mL), and the presence of the free amino groups was checked with the TNBS test. *Peptide coupling*: A preformed solution of Fmoc-Arg(Pmc)-OH (457 mg, 0.69 mmol), TBTU (176 mg, 0.55 mmol), HOBt (93 mg, 0.69 mmol), and DIEA (241 μL, 1.38 mmol) in NMP (2.5 mL) was added to the deprotected peptidyl resin. The mixture was shaken at room temperature for 1.5 h. Completion of the reaction was checked with the TNBS test. The solution was drained and the resin was washed several times with DMF (3 × 3 mL), *i*-PrOH (3 × 3 mL), Et_2O (2 × 3 mL), and DCM (3 × 3 mL). The resin was washed again with DMF (5 × 3 mL) and then treated with 20% v/v piperidine in DMF (5 mL × 5 min × 6 cycles). The solution was drained, the resin was washed with DMF (5 × 3 mL), *i*-PrOH (3 × 3 mL), Et_2O (2 × 3 mL), DCM (2 × 3 mL), and DMF (2 × 3 mL), and the presence of the free amino groups was checked with the TNBS test.

The coupling of the aminoproline module **21** (Amp**21**; 250 mg, 0.55 mmol) and Fmoc-Asp(Bu^t)-OH (283 mg, 0.69 mmol) residues was carried out under the same conditions. *Resin cleavage*: The resin-bound peptide, H-Asp(Bu^t)-Amp**21**-Arg(Pmc)-Gly-O-cTrt, was treated with 5 mL of a mixture of hexafluoroisopropanol (HFIP) and DCM (1:4) for 15 min at ambient temperature. The solution was recovered and the resin was carefully washed with the above HFIP/DCM mixture (2 × 5 mL × 10 min). The combined solution was coevaporated under vacuum with hexane several times, furnishing the linear tetrapeptide H-Asp(Bu^t)-Amp**21**-Arg(Pmc)-Gly-OH (114 mg, 47%) as a white solid, used as such in the subsequent synthesis step.

In-Solution Synthesis and Analysis. *Cyclization*: The linear tetrapeptide H-Asp(Bu^t)-Amp**21**-Arg(Pmc)-Gly-OH (114 mg, 0.13 mmol) was dissolved in DMF (37 mL) under nitrogen at room temperature. HATU (148 mg, 0.39 mmol), HOAt (0.6 M solution in DMF, 650 μL, 0.39 mmol), and 2,4,6-collidine (52 μL, 0.39 mmol) were added, and the reaction mixture was stirred at ambient temperature for 24 h. The reaction mixture was concentrated under vacuum, the solid residue was dissolved in EtOAc (8 mL), and the solution was washed with 5% aqueous $NaHCO_3$. The organic layers were collected, dried over $MgSO_4$, filtered, and evaporated under vacuum to afford a crude residue that was purified by flash chromatography (EtOAc/MeOH 8:2), furnishing the protected cyclic tetrapeptide (84 mg, 75%) as a glassy white solid. *Side chain deprotection*: The protected cyclic tetrapeptide (84 mg, 0.097 mmol) was treated with 5 mL of a solution of TFA/TIS/H_2O 95:2.5:2.5 at ambient temperature. After 24 h, the solvent was evaporated under vacuum and the residue was dissolved in 5 mL of 3 N aq HCl and thoroughly washed with Et_2O (4×). The aqueous phase was concentrated under vacuum furnishing the deprotected cyclic tetrapeptide, *cyclo*-[-Arg-Gly-Asp-Amp**21**-] (**5**; 46 mg, quant., corresponding to an overall yield of 35%), as a hydrochloride salt. *Peptide purification*: The final product was dissolved in 5 mL of HPLC grade H_2O and filtered with a 0.2 μm, 100 mm Anotop 10 LC filter (Whatman). The cyclic tetrapeptide was purified by semipreparative RP-HPLC (RP C18-10 μm, 250 × 10 mm) using acetonitrile (0.05% TFA) in H_2O (0.05% TFA), 0–35% linear gradient over 25 min at room temperature. A flow rate of 5.0 mL/min was used and detection was at 220 nm. HPLC R_t = 5.8 min. Purity of final cyclopeptide was checked with analytical HPLC (Discovery C18-10 μm column, 250 × 4.6 mm) in two different solvent systems (methanol/water and acetonitrile/water) using a gradient program and found to be >98% pure. The HPLC sample was evaporated under vacuum and finally transformed into the hydrochloride salt by exposing the solid material to anhydrous gaseous HCl until constant weight was reached, ready for biological assay. A glassy solid; $[\alpha]_D^{25}$ –5.80 (*c* 0.62, H_2O; HCl salt); ^{1}H NMR (800 MHz, H_2O/D_2O 9:1, 298 K) δ 9.07 (NH Gly), 8.90 ($J_{NH,\alpha}$ = 5.50 Hz, NH Arg), 8.51 ($J_{NH,\alpha}$ = 8.98 Hz, NH Asp), 7.30 ($J_{NH,\gamma}$ = 5.40 Hz, NH Amp), 7.20 (NHϵ Arg), 4.73 (Hα Asp), 4.67 (H2 Amp), 4.51 (H4 Amp), 4.25 (Hα Arg), 4.13 and 3.56 (Hα Gly), 3.72 and 3.68 (H5 Amp), 3.24 (Hδ Arg), 2.94 (Hβ Asp), 2.77 and 2.48 (H3 Amp), 1.79 and 1.73 (Hβ Arg), 1.73 and 1.65

(Hγ Arg); ^{13}C NMR (200 MHz, H_2O/D_2O 9:1, 298 K) δ 59.0 (*C*2 Amp), 58.20 (Cα Arg), 55.30 (C5 Amp), 52.33 (C4 Amp), 47.40 (Cα Gly), 43.40 (Cδ Arg), 38.70 (C3 Amp), 37.80 (Cβ Asp), 29.30 (Cβ Arg), 27.20 (Cγ Arg). HRMS (ES+) $C_{17}H_{29}N_8O_6$ calcd for $[MH]^+$, 441.2205; found, 441.2184. Anal. ($C_{17}H_{28}N_8O_6 \cdot HCl$) C, H, N.

***cyclo*-[-Arg-Gly-Asp-Amp25-] (6).** Cyclopeptide **6** was prepared according to the procedure described for **5** and utilizing aminoproline module **25** (Amp**25**; 250 mg, 0.55 mmol) in place of **21**. Overall yield: 26% (34 mg). A glassy solid; $[\alpha]_D^{25}$ –20.37 (*c* 0.36, H_2O) (HCl salt); HPLC purity: >98%; RP-HPLC (RP C18–10μm, 250 × 10 mm) using acetonitrile (0.05% TFA) in H_2O (0.05% TFA), 0–35% linear gradient over 25 min; flow rate 5.0 mL/min, detection at 220 nm, R_t = 6.4 min.; ^{1}H NMR (800 MHz, H_2O/D_2O 9:1, 298K) δ 8.83 ($J_{NH,\alpha}$ = 7.06 Hz, NH Arg), 8.67 (NH Gly), 8.38 ($J_{NH,\alpha}$ = 7.29 Hz, NH Asp), 8.19 ($J_{NH,\gamma}$ = 6.20 Hz, NH Amp), 7.20 (NHε Arg), 4.70 (H2 Amp), 4.60 (Hα Asp), 4.46 (H4 Amp), 4.43 (Hα Arg), 4.09 and 3.81 (Hα Gly), 3.78 and 3.35 (H5 Amp), 3.22 (Hδ Arg), 2.87 (Hβ Asp), 2.50 and 2.44 (H3 Amp), 1.87 and 1.79 (Hβ Arg), 1.64 (Hγ Arg); ^{13}C NMR (200 MHz, H_2O/D_2O 9:1, 298 K) δ 56.37 (Cα Arg), 53.34 (Cα Asp), 52.72 (C5 Amp), 51.80 (C4 Amp), 45.57 (Cα Gly), 43.40 (Cδ Arg), 38.74 (Cβ Asp), 37.26 (C3 Amp), 30.90 (Cβ Arg), 27.17 (Cγ Arg). HRMS (ES+) $C_{17}H_{29}N_8O_6$ calcd for $[MH]^+$, 441.2205; found, 441.2239. Anal. ($C_{17}H_{28}N_8O_6 \cdot HCl$) C, H, N.

***cyclo*-[-Arg-Gly-Asp-Amp28-] (7).** Cyclopeptide **7** was prepared according to the procedure described for **5** and utilizing aminoproline module **28** (Amp**28**; 220 mg, 0.49 mmol) in place of **21**. Overall yield: 30% (35 mg). A glassy solid; $[\alpha]_D^{25}$ +4.53 (*c* 0.38, H_2O; HCl salt); HPLC purity ≥ 98%; RP-HPLC (RP C18–10μm, 250 × 10 mm) using acetonitrile (0.05% TFA) in H_2O (0.05% TFA), 0–25% linear gradient over 25 min; flow rate 5.0 mL/min, detection at 220 nm, R_t = 6.2 min; ^{1}H NMR (800 MHz, H_2O/D_2O 9:1, 298 K) δ 9.31 ($J_{NH,\alpha}$ = 6.44 Hz, NH Arg), 8.66 (NH Gly), 7.83 ($J_{NH,\alpha}$ = 8.66 Hz, NH Asp), 7.18 (NHε Arg), 6.89 ($J_{NH,\gamma}$ = 4.86 Hz, NH Amp), 4.78 (Hα Asp), 4.68 (H2 Amp), 4.44 (H4 Amp), 4.12 and 3.71 (Hα Gly), 3.88 (Hα Arg), 3.77 and 3.55 (H5 Amp), 3.24 (Hδ Arg), 2.95 and 2.78 (Hβ Asp), 2.71 and 2.47 (H3 Amp), 2.14 and 1.97 (Hβ Arg), 1.70 and 1.63 (Hγ Arg); ^{13}C NMR (200 MHz, H_2O/D_2O 9:1, 298 K) δ 58.80 (C2 Amp), 58.77 (Cα Arg), 54.75 (C5 Amp), 52.72 (C4 Amp), 47.45 (Cα Gly), 43.47 (Cδ Arg), 38.64 (Cβ Asp), 38.12 (C3 Amp), 27.72 (Cβ Arg), 27.62 (Cγ Arg). HRMS (ES+) $C_{17}H_{29}N_8O_6$ calcd for $[MH]^+$, 440.2205; found, 440.2218. Anal. ($C_{17}H_{28}N_8O_6 \cdot HCl$) C, H, N.

***cyclo*-[-Arg-Gly-Asp-Amp27-] (8).** Cyclopeptide **8** was prepared according to the procedure described for **5** and utilizing aminoproline module **27** (Amp**27**; 211 mg, 0.47 mmol) in place of **21**. Overall yield: 29% (32 mg). A glassy solid; $[\alpha]_D^{25}$ –3.6 (*c* 0.33, H_2O; HCl salt); HPLC purity ≥ 98%; RP-HPLC (RP C18-10 μm, 250 × 10 mm) using acetonitrile (0.05% TFA) in H_2O (0.05% TFA), 0–25% linear gradient over 25 min; flow rate 5.0 mL/min, detection at 220 nm, R_t = 9.2 min.; ^{1}H NMR (800 MHz, H_2O/D_2O 9:1, 298 K) δ 8.93 ($J_{NH,\alpha}$ = 6.52 Hz, NH Arg), 8.67 (NH Gly), 8.39 ($J_{NH,\gamma}$ = 6.23 Hz, NH Amp), 8.22 ($J_{NH,\alpha}$ = 7.19 Hz, NH Asp), 7.22 (NHε Arg), 4.66 (H2 Amp), 4.60 (Hα Asp), 4.52 (H4 Amp), 4.38 (Hα Arg), 4.01 and 3.90 (Hα Gly), 3.74 and 3.42 (H5 Amp), 3.20 (Hδ Arg), 2.79 (Hβ Asp), 2.51 and 2.41 (H3 Amp), 1.89 and 1.79 (Hβ Arg), 1.63 (Hγ Arg); ^{13}C NMR (200 MHz, H_2O/D_2O 9:1, 298 K) δ 56.90 (Cα Arg), 53.34 (Cα Asp), 52.72 (C5 Amp), 51.80 (C4 Amp), 45.60 (Cα Gly), 43.34 (Cδ Arg), 39.77 (Cβ Asp), 37.80 (C3 Amp), 30.80 (Cβ Arg), 27.20 (Cγ Arg). HRMS (ES+) $C_{17}H_{29}N_8O_6$ calcd for $[MH]^+$, 441.2205; found, 441.2178. Anal. ($C_{17}H_{28}N_8O_6 \cdot HCl$) C, H, N.

***cyclo*-[-Arg-Gly-Asp-Amp24-] (9).** Cyclopeptide **9** was prepared according to the procedure described for **5** and utilizing aminoproline module **24** (Amp**24**; 238 mg, 0.53 mmol) in place of **21**. Overall yield: 27% (41 mg). A glassy solid; $[\alpha]_D^{25}$ –19.06 (*c* 0.34, H_2O; HCl salt); HPLC purity ≥ 98%; RP-HPLC (RP C18-10 μm, 250 × 10 mm) using acetonitrile (0.05% TFA) in H_2O (0.05% TFA), 0–35% linear gradient over 25 min; flow rate 5.0 mL/min, detection at 220 nm, R_t = 17.0 min.; ^{1}H NMR (800 MHz, H_2O/D_2O 9:1, 298 K) δ 9.11 (NH Gly), 9.04 ($J_{NH,\alpha}$ = 3.60 Hz, NH Arg), 8.58 ($J_{NH,\alpha}$ = 8.83 Hz, NH Asp), 7.28 ($J_{NH,\gamma}$ not determined, NH Amp), 7.23 (NHε Arg), 4.76 (Hα Asp), 4.65 (H2 Amp), 4.44 (H4 Amp), 4.29 (Hα Arg), 4.13 and 3.61 (Hα Gly), 4.07 and 3.54 (H5 Amp), 3.31 (H1′), 3.27 (Hδ Arg), 2.98 and 2.54 (H3 Amp), 2.93 (Hβ Asp), 1.82 (Hβ Arg), 1.76 and 1.69 (Hγ Arg), 1.62 (H2′), 1.31 (H3′), 1.29 (H4′), 1.26 (H6′), 1.25 (H5′), 0.88 (H7′); ^{13}C NMR (200 MHz, H_2O/D_2O 9:1, 298 K) δ 58.73 (Cα Arg), 58.40 (C1′), 53.34 (Cα Asp), 52.72 (C5 Amp), 52.50 (C4 Amp), 47.41 (Cα Gly), 43.45 (Cδ Arg), 38.12 (Cβ Asp), 37.74 (C3 Amp), 33.43 (*C*2′), 30.58 (C3′), 29.25 (Cβ Arg), 28.26 (C5′), 27.72 (C4′), 27.25 (Cγ Arg), 24.58 (C6′), 16.30 (C7′); ^{15}N NMR (60 MHz, H_2O/D_2O 9:1, 298 K) γ 126.9 (Asp), 122.1 (Arg), 121.4 (Amp), 118.5 (Gly). HRMS (ES+) $C_{24}H_{43}N_8O_6$ calcd for $[MH]^+$, 539.3300; found, 539.3277. Anal. ($C_{24}H_{42}N_8O_6 \cdot HCl$) C, H, N.

***cyclo*-[-Arg-Gly-Asp-Amp23-] (10).** Cyclopeptide **10** was prepared according to the procedure described for **5** and utilizing aminoproline module **23** (Amp**23**; 204 mg, 0.50 mmol) in place of **21**. Overall yield: 23% (30 mg). A glassy solid; $[\alpha]_D^{25}$ –14.5 (*c* 0.68, H_2O; HCl salt); HPLC purity ≥ 98%; RP-HPLC (RP C18-10 μm, 250 × 10 mm) using acetonitrile (0.05% TFA) in H_2O (0.05% TFA), 0–25% linear gradient over 25 min; flow rate 5.0 mL/min, detection at 254 nm, R_t = 9.2 and 9.4 min.; ^{1}H NMR (800 MHz, H_2O/D_2O 9:1, 298 K, 85:15 mixture of ^{A}*trans*/^{B}*cis* isomers) δ 8.91 (NH Gly_B), 8.84 (NH Gly_A), 8.80 ($J_{NH,\alpha}$ not determined, NH Arg_B), 8.70 ($J_{NH,\alpha}$ = 4.60 Hz, NH Arg_A), 8.26 ($J_{NH,\alpha}$ = 9.00 Hz, NH $Asp_{A,B}$), 7.38 ($J_{NH,\gamma}$ = 7.63 Hz, NH Amp_A), 7.30 ($J_{NH,\gamma}$ not determined, NH Amp_B), 7.13 (NHε $Arg_{A,B}$), 4.67 (Hα $Asp_{A,B}$), 4.59 (H2 Amp_A), 4.50 (H4 Amp_A), 4.42 (H4 Amp_B), 4.11 (Hα Arg_B), 4.10 and 3.48 (Hα Gly_B), 4.08 and 3.49 (Hα Gly_A), 4.07 (Hα Arg_A), 3.88 and 3.63 (H5 Amp_A), 3.77 and 3.55 (H5 Amp_B), 3.18 (Hδ $Arg_{A,B}$), 2.84 (Hβ $Asp_{A,B}$), 2.68 and 2.18 (H3 Amp_B), 2.54 and 2.04 (H3 Amp_A), 2.33 ($H2'_A$), 2.23 and 2.03 ($H2'_B$), 1.73 (Hβ $Arg_{A,B}$), 1.58 (Hγ Arg_A), 1.57 (Hγ Arg_B), 1.00 ($H3'_A$), 0.97 ($H3'_B$); ^{13}C NMR (200 MHz, H_2O/D_2O 9:1, 298 K) δ 56.60 (C5 Amp_B), 56.40 (C5 Amp_A), 47.22 (Cα $Gly_{A,B}$), 43.47 (Cδ $Arg_{A,B}$), 39.53 (C3 Amp_B), 37.77 (Cβ $Asp_{A,B}$), 37.63 (C3 Amp_A), 30.03 ($C2'_A$), 30.00 ($C2'_B$), 29.19 (Cβ $Arg_{A,B}$), 27.23 (Cγ $Arg_{A,B}$), 11.28 ($C3'_B$), 10.89 ($C3'_A$); ^{15}N NMR (60 MHz, H_2O/D_2O 9:1, 298 K) γ 130.13 (Amp_B), 129.70 (Amp_A), 124.8 ($Asp_{A,B}$), 124.0 (Arg_B), 123.5 (Arg_A), 117.81 (Gly_B), 117.30 (Gly_A). HRMS (ES+) $C_{20}H_{33}N_8O_7$ calcd for $[MH]^+$, 497.2472; found, 497.2450. Anal. ($C_{20}H_{32}N_8O_7 \cdot HCl$) C, H, N.

***cyclo*-[-Arg-Gly-Asp-Amp22-] (11).** Cyclopeptide **11** was prepared according to the procedure described for **5** and utilizing aminoproline module **22** (Amp**22**; 250 mg, 0.55 mmol) in place of **21**. Overall yield: 31% (49 mg). A glassy solid; $[\alpha]_D^{25}$ –8.56 (*c* 0.66, H_2O; HCl salt); HPLC purity ≥ 98%; RP-HPLC (RP C18-10 μm, 250 × 10 mm) using acetonitrile (0.05% TFA) in H_2O (0.05% TFA), 0–35% linear gradient over 25 min; flow rate 5.0 mL/min, detection at 254 nm, R_t = 11.8 min. ^{1}H NMR (800 MHz, H_2O/D_2O 9:1, 298 K, 54:46 mixture of ^{A}*cis*/^{B}*trans* isomers) δ 8.94 (NH Gly_A), 8.86 ($J_{NH,\alpha}$ = 4.56 Hz, NH Arg_A), 8.76 (NH Gly_B), 8.46 ($J_{NH,\alpha}$ = 4.60 Hz, NH Arg_B), 8.31 ($J_{NH,\alpha}$ = 8.96 Hz, NH $Asp_{A,B}$), 7.53 ($J_{NH,\gamma}$ not determined, NH Amp_B), 7.51 (Hε $Ph_{A,B}$), 7.50 ($J_{NH,\gamma}$ not determined, NH Amp_A), 7.48 (Hξ, $Ph_{A,B}$), 7.32 (Hδ $Ph_{A,B}$), 7.20 (NHε Arg_A), 7.14 (NHε Arg_B), 4.82 ($H2_{A,B}$ Amp), 4.68 (Hα $Asp_{A,B}$), 4.65 (H4 Amp_B), 4.52 (H4 Amp_A), 4.17 (Hα Arg_A), 4.14 and 3.56 (Hα Gly_A), 4.08 and 3.57 (Hα Gly_B), 4.06 and 3.81 (H5 Amp_B), 4.01 and 3.53 (H5 Amp_A), 3.88 (Hα Arg_B), 3.26 (Hδ Arg_A), 3.12 (Hδ Arg_B), 2.86 (Hβ $Asp_{A,B}$), 2.72 and 2.16 (H3 Amp_A), 2.70 and 2.06 (H3 Amp_B), 1.81 (Hβ Arg_A), 1.66 (Hγ Arg_A), 1.62 (Hβ Arg_B), 1.48 (Hγ Arg_B); ^{13}C NMR (200 MHz, H_2O/D_2O 9:1, 298 K) δ 129.81 (Cξ, $Ph_{A,B}$), 128.62 (Cε, $Ph_{A,B}$), 127.23 (Cδ, $Ph_{A,B}$), 54.72 (C5 Amp_A), 54.18 (Cα Arg_A), 53.80 (Cα Arg_B), 52.30 (C5 Amp_B), 48.34 (Cα $Asp_{A,B}$), 48.30 (C4 $Amp_{A,B}$), 43.00 (Cα Gly_A), 42.90 (Cα Gly_B), 39.22 (Cδ Arg_A), 39.00 (Cδ Arg_B), 35.30 (C3 Amp_B), 33.60 (C3 Amp_A), 33.50 (Cβ $Asp_{A,B}$), 25.05 (Cβ Arg_A), 24.70 (Cβ Arg_B), 23.05 (Cγ Arg_B), 23.00 (Cγ Arg_A). HRMS (ES+) $C_{24}H_{33}N_8O_7$ calcd for $[MH]^+$, 545.2467; found, 545.2488. Anal. ($C_{24}H_{32}N_8O_7 \cdot HCl$) C, H, N.

***cyclo*-[-Arg-Gly-Asp-Amp26-] (12).** Cyclopeptide **12** was prepared according to the procedure described for **5** and utilizing aminoproline module **26** (Amp**26**; 196 mg, 0.43 mmol) in place of **21**. Overall yield: 27% (34 mg). A glassy solid; $[\alpha]_D^{25}$ –22.1 (*c* 0.2, H_2O; HCl salt); HPLC purity ≥ 98%; RP-HPLC (RP C18-10 μm, 250 × 10 mm) using acetonitrile (0.05% TFA) in H_2O (0.05% TFA), 0–25% linear gradient over 25 min; flow rate 5.0 mL/min, detection at 254 nm, R_t = 16.9 min. ^{1}H NMR (600 MHz, H_2O/D_2O 9:1, 298 K, mixture of three isomers, two major isomers) δ 8.69 (NH Gly_A), 8.65 (NH Gly_B), 8.61 ($J_{NH,\alpha}$ = 8.57 Hz, NH $Arg_{A,B}$), 8.46 ($J_{NH,\alpha}$ = 8.41 Hz, NH $Asp_{A,B}$), 8.04 ($J_{NH,\gamma}$ = 7.72 Hz, NH $Amp_{A,B}$), 7.78 (Hδ $Ph_{A,B}$), 7.72 (Hϵ $Ph_{A,B}$), 7.62 (Hξ, $Ph_{A,B}$), 7.55 (NHϵ Arg_A), 7.19 (NHϵ Arg_B), 4.78 (H2 $Amp_{A,B}$), 4.55 (Hα Asp_B), 4.53 (Hα Arg_A), 4.49 (Hα Arg_B), 4.47 (Hα Asp_A), 4.37 (H4 Amp_A), 4.36 (H4 Amp_B), 4.07 and 3.81 (Hα Gly_B), 3.97 and 3.84 (Hα Gly_A), 3.95 and 3.69 (H5 Amp_A), 3.87 and 3.62 (H5 Amp_B), 3.19 (Hδ Arg_B), 3.13 (Hδ Arg_A), 2.78 (Hβ Asp_B), 2.70 (Hβ Asp_A), 2.51 and 2.21 (H3 Amp_A), 2.50 and 2.33 (H3 Amp_B), 1.99 (Hβ Arg_A), 1.86 (Hβ Arg_B), 1.83 and 1.70 (Hγ Arg_A), 1.67 (Hγ Arg_B); ^{13}C NMR (200 MHz, H_2O/D_2O 9:1, 298 K, major isomer) δ 129.80 (Cξ, Ph), 128.51 (Cϵ, Ph), 127.04 (Cδ, Ph), 55.00 (C5 Amp), 54.15 (Cα Arg), 48.44 (Cα Asp), 48.30 (C4 Amp), 43.21 (Cα Gly), 39.55 (Cδ Arg), 35.42 (C3 Amp), 33.50 (Cβ Asp), 25.05 (Cβ Arg), 23.00 (Cγ Arg); ^{15}N NMR (60 MHz, H_2O/D_2O 9:1, 298 K, major isomer) γ 122.8 (Amp), 122.6 (Arg), 119.3 (Asp), 110.7 (Gly). HRMS (ES+) $C_{24}H_{33}N_8O_7$ calcd for $[MH]^+$, 545.2467; found, 545.2501. Anal. ($C_{24}H_{32}N_8O_7 \cdot HCl$) C, H, N.

Solid-Phase Receptor Binding Assay. [^{125}I]-Echistatin, labeled by the lactoperoxidase method[32] to a specific activity of 2000 Ci/mmol, was purchased from GE Healthcare. Integrin proteins $\alpha_V\beta_3$ and $\alpha_V\beta_5$ purified from human placenta were purchased from Chemicon International Inc., Temecula, CA. The receptor binding assay was performed as described.[18a,b,33] Purified receptors $\alpha_V\beta_3$ and $\alpha_V\beta_5$ were diluted respectively at 500 ng/mL and 1000 ng/mL in coating buffer [20 mM Tris (pH 7.4), 150 mM NaCl, 2 mM $CaCl_2$, 1 mM $MgCl_2$, 1 mM $MnCl_2$]. An aliquot of the diluted receptors (100 μL/well) was added to a 96-well microtiter plate (Optiplate-96 HB, PerkinElmer Life Sciences, Boston, MA) and incubated overnight at 4 °C. The plate was washed once with blocking/binding buffer [20 mM Tris (pH 7.4), 150 mM NaCl, 2 mM $CaCl_2$, 1 mM $MgCl_2$, 1 mM $MnCl_2$, 1% BSA] and incubated an additional 2 h at room temperature. The plate was rinsed twice with the same buffer, then competition binding studies were performed with a fixed concentration of [^{125}I]-echistatin (0.05 nM and 0.1 nM for $\alpha_V\beta_3$ and $\alpha_V\beta_5$, respectively) and concentrations ranging from 0.01 nM and 100 μM of the tested compounds. All assays were performed in triplicate in a final volume of 0.2 mL, each containing the following species: 0.05 mL of [^{125}I]-echistatin, 0.04 mL of the tested compound and 0.11 mL of blocking/binding buffer. Nonspecific binding was defined as [^{125}I]-echistatin bound in the presence of an excess (1 μM) of unlabeled echistatin. After incubation for 3 h at room temperature, the plate was washed three times with blocking/binding buffer, then counted in a Top-Count NXT microplate scintillation counter (PerkinElmer Life Sciences, Boston, MA) using 200 μL/well of MicroScint-40 liquid scintillation (PerkinElmer Life Sciences, Boston, MA).

Biological Data Analysis. The IC_{50} values were determined by fitting binding inhibition data by nonlinear regression using GraphPad Prism 4.0 Software Package (GraphPad Prism, San Diego, CA). Moreover, when the Hill slope of the curves was significantly less the unity (K < –0.80), the data were reanalyzed with a two-site model. The displacement curves better fitted (p < 0.05) by a two-site model than one-site model were considered significant.

NMR Spectroscopy. For NMR experiments of compounds **5**−**12**, the samples were dissolved in H_2O/D_2O (90%/10%) at a concentration of 5–10 mM. The NMR measurements were performed at 25 °C with a 600 MHz and/or 800 MHz Varian-INOVA spectrometers. To assign the proton resonances, conventional 2D experiments, such as TOCSY, NOESY, and ROESY, were recorded. TOCSY spectra were acquired using an MLEV-17 spin-lock sequence at a field strength of 10 kHz and an evolution time of 80 ms. NOESY experiments were carried out with mixing times of 200 and 400 ms. ROESY spectra were also collected, using a continuous wave mixing of 200 and 400 ms (3.0 kHz spin-locking field strength). All 2D experiments were acquired in the phase-sensitive mode using a reported method.[34] In all spectra, water suppression was achieved using the WATERGATE technique. The cross-peak intensities were measured from the ROESY spectra with a mixing time of 200 ms. No differences were observed in the ROESY spectra with different mixing times. To relate the ROEs data with the interproton distances, the calibration was made using the distance of 1.8 Å for the well-defined geminal β-protons. The ROE intensities were classified as strong, medium, and weak, corresponding to upper bound distance constraints of 2.7, 3.5, and 5.0 Å, respectively. Lower bounds between nonbonded atoms were set to the sum of their van der Waals radii (1.8 Å). Side-chain protons were not stereospecifically assigned, hence, ROE restraints for the side-chain protons were calculated by considering pseudo atoms.[35]

Constraints for the dihedral angles were deduced on the basis of $^3J_{NH\text{-}\alpha H}$ coupling constants from the 1D spectrum and were calculated using the J values extracted by solving the Karplus equation. The temperature coefficients of the amide proton chemical shifts were calculated from 1D ^{1}H NMR experiments performed at different temperatures in the range 5–40 °C by means of linear regression.

The quality of the final structures was verified on the basis of the minimum number of ROE distance violations, ideal bond geometry, van der Waals contacts, and analysis of the Φ and Ψ dihedral angles. The degree of convergence of the structures was judged by examining the pairwise root-mean-square-deviation values for the backbone atoms. The lowest energy structure was chosen from this family as a representative structure.

Structure Calculations. Solution structures were calculated using the simulated annealing method as previously described.[7g] A total of ∼40 ROE-derived distance restraints and three dihedral angle restraints were used to determine the structures. For each examined peptide, an ensemble of 100 structures was generated. Solution structures that had the lowest overall energies and no constraint violations were selected and analyzed. All of the structures were displayed and further analyzed using the InsightII program (Accelerys, Inc., San Diego, CA).

Docking Simulations. Automated docking studies were performed by means of the AutoDock 4.0.1 program.[28] AutoDock is a fully automated docking suite of programs that employs a Lamarckian genetic algorithm (LGA) as a search engine. Three-dimensional energy scoring grids of 0.375 Å resolution and 100 Å × 100 Å × 100 Å dimensions were computed. The center of the grid was set to be coincident with the mass center of the ligands. A total of 50 runs with a maximum of 2.5 M energy evaluations were performed for each ligand. The default parameters for the LGA were used. The AutoDockTool (ADT) graphical interface[36] was used to prepare the receptor and the ligands PDBQT files. The coordinates of the analyzed ligands were retrieved from the NMR-determined structures, while the coordinates of ligated **1** was retrieved from the Protein Data Bank (code 1L5G; the protein was unmerged from the complex of protein and ligand). Water molecules were removed. For the protein receptor, polar hydrogens were added and Kollman charges were assigned. For the cyclopeptide ligands, all the hydrogens were used with Kollman charges. Cluster analysis was performed on the docked results using a root-mean-square tolerance (rms) of 1.5 Å. The mode of interaction of the native ligand within the $\alpha_V\beta_3$ receptor was used for rmsd calculation.

Acknowledgment. This work was supported by Ministero dell'Istruzione, dell'Università e della Ricerca (PRIN 2006, Roma, Italy). We thank the Centro Interdipartimentale Misure "G. Casnati" (Università di Parma) and the NMR Centre of Mill Hill at the National Institute for Medical Research, London (UK) for instrumental facilities. Thanks are due to Flamma Spa (Italy)

for the generous gift of *cis*-*N*-Boc-4-hydroxy-D-proline. A postdoctoral fellowship to P.B. from Centro Interdisciplinare di Studi Bio-Molecolari e Applicazioni Industriali (CISI, Milano, Italy) is gratefully acknowledged.

Supporting Information Available: General methods, experimental procedures, and spectroscopic data for compounds **15**−**28**, elemental analyses of intermediary and target compounds (Table S1), reproductions of ^{1}H NMR spectra of cyclopeptides **5**−**12** (Figures S1−S8), concentration–response curves of cyclopeptides **5**−**12** to $\alpha_V\beta_3$ and $\alpha_V\beta_5$ receptors (Figure S9−S16), schematic 2D view of interactions between **9** and $\alpha_V\beta_3$ (Figure S17), and additional presentations of molecular docking (Figures S18 and S19). This material is available free of charge via the Internet at http://pubs.acs.org.

References

(1) (a) Leading references: Hynes, R. O. Integrins: A family of cell surface receptors. *Cell* **1987**, *48*, 549–554. (b) Hynes, R. O. Integrins: Versatility, modulation, and signalling in cell adhesion. *Cell* **1992**, *69*, 11–25. (c) Cox, D.; Aoki, T.; Seki, J.; Motoyama, Y.; Yoshida, K. The pharmacology of the integrins. *Med. Res. Rev.* **1994**, *14*, 195–228. (d) Aplin, A. E.; Howe, A.; Alahari, S. K.; Juliano, R. L. Signal transduction and signal modulation by cell adhesion receptors: the role of integrins, cadherins, immunoglobulin-cell adhesion molecules, and selectins. *Pharmacol. Rev.* **1998**, *50*, 197–264. (e) Giancotti, F. G.; Ruoslahti, E. Integrin signaling. *Science* **1999**, *285*, 1028–1032. (f) Hynes, R. O. Integrins: Bidirectional, allosteric signalling machines. *Cell* **2002**, *110*, 673–687. (g) Springer, T. A.; Wang, J.-H. In *Cell Surface Receptors*; Garcia, K. C. Ed.; Elsevier: San Diego, 2004.

(2) (a) Ruoslahti, E.; Pierschbacher, M. D. Arg-Gly-Asp: A versatile cell recognition signal. *Cell* **1986**, *44*, 517–518. (b) Ruoslahti, E. The RGD story: A personal account. *Matrix Biol.* **2003**, *22*, 459–465.

(3) (a) Varner, J. A.; Cheresh, D. A. Tumor angiogenesis and the role of vascular cell integrin $\alpha_V\beta_3$. *Adv. Oncol.* **1996**, 69–87. (b) Arndt, T.; Arndt, U.; Reuning, U.; Kessler, H. Integrins in angiogenesis: Implications for tumor therapy. In *Cancer Therapy: Molecular Targets in Tumor-Host Interactions*; Weber, G. F., Ed.; Horizon Bioscience, Cromwell Press: Wymondham, Norfolk, U. K., 2005, 93–141. (c) Danem, E. H. J. Integrins: Regulators of tissue function and cancer progression. *Curr. Pharm. Des.* **2005**, *11*, 881–891. (d) Meyer, A.; Auernheimer, J.; Modlinger, A.; Kessler, H. Targeting RGD recognizing integrins: Drug development, biomaterial research, tumor imaging and targeting. *Curr. Pharm. Des.* **2006**, *12*, 2723–2747.

(4) (a) Hood, J. D.; Cheresh, D. A. Role of integrins in cell invasion and migration. *Nat. Rev. Cancer* **2002**, *2*, 91–100. (b) Alghisi, G. C.; Rüegg, C. Vascular integrins in tumor angiogenesis: Mediators and therapeutic targets. *Endothelium* **2006**, *13*, 113–135.

(5) (a) Friedlander, M.; Brooks, P. C.; Shaffer, R. W.; Kincaid, C. M.; Varner, J. A.; Cheresh, D. A. Definition of two angiogenic pathways by distinct α_V integrins. *Science* **1995**, *270*, 1500–1502. (b) Brooks, P. C.; Klemke, R. L.; Schon, S.; Lewis, J. M.; Schwartz, M. A.; Cheresh, D. A. Insulin-like growth factor receptor cooperates with integrin $\alpha_V\beta_5$ to promote tumor cell dissemination in vivo. *J. Clin. Invest.* **1997**, *99*, 1390–1398.

(6) (a) The involvement of the $\alpha_V\beta_3$ and/or $\alpha_V\beta_5$ integrins in other critical processes, such as osteoclasts-to-bone adhesion and vascular smooth muscle migration also suggests the potential therapeutic significance of efficient ligand antagonists in bone pathologies (osteoporosis), atherosclerotic vascular damage, restenosis after coronary angioplasty, rheumatoid arthritis, and ocular diseases. See, for example: Rodan, S. B.; Rodan, G. A. Integrin function in osteoclasts. *J. Endocrinol.* **1997**, *154*, S47–S56. (b) Storgard, C. M.; Stupack, D. G.; Jonczyk, A.; Goodman, S. L.; Fox, R. I.; Cheresh, D. A. Decreased angiogenesis and arthritic disease in rabbits treated with an $\alpha_V\beta_3$ antagonist. *J. Clin. Invest.* **1999**, *103*, 47–54. (c) Teitelbaum, S. L. Osteoclasts, integrins, and osteoporosis. *J. Bone Miner. Metab.* **2000**, *18*, 344–349. (d) Rüegg, C.; Mariotti, A. Vascular integrins: Pleiotropic adhesion and signaling molecules in vascular homeostasis and angiogenesis. *Cell. Mol. Life Sci.* **2003**, *60*, 1135–1157.

(7) (a) Ojima, I.; Chakravarty, S.; Dong, Q. Antithrombotic agents: From RGD to peptide mimetics. *Bioorg. Med. Chem.* **1995**, *3*, 337–360. (b) Wermuth, J.; Goodman, S. L.; Jonczyk, A.; Kessler, H. Stereoisomerism and biological activity of the selective and superactive $\alpha_V\beta_3$ integrin inhibitor cyclo(-RGDfV-) and its retroinverso peptide. *J. Am. Chem. Soc.* **1997**, *119*, 1328–1335. (c) Dechantsreiter, M. A.; Planker, E.; Mathä, B.; Lohof, E.; Hölzemann, G.; Jonczyk, A.; Goodman, S. L.; Kessler, H. N-Methylated cyclic RGD peptides as highly active and selective $\alpha_V\beta_3$ integrin antagonists. *J. Med. Chem.* **1999**, *42*, 3033–3040. (d) Miller, W. H.; Keenan, R. M.; Willette, R. N.; Lark, M. W. Identification and in vivo efficacy of small-molecule antagonists of integrin $\alpha_V\beta_3$ (the vitronectin receptor). *Drug Discovery Today* **2000**, *5*, 397–408. (e) Belvisi, L.; Bernardi, A.; Checchia, A.; Manzoni, L.; Potenza, D.; Scolastico, C.; Castorina, M.; Cupelli, A.; Giannini, G.; Carminati, P.; Pisano, C. Potent integrin anatagonists from a small library of RGD-including cyclic pseudopeptides. *Org. Lett.* **2001**, *3*, 1001–1004. (f) Cardo-Vila, M.; Arap, W.; Pasqualini, R. $\alpha_V\beta_5$ Integrin-dependent programmed cell death triggered by a peptide mimic of annexin V. *Mol. Cell* **2003**, *11*, 1151–1162. (g) Casiraghi, G.; Rassu, G.; Auzzas, L.; Burreddu, P.; Gaetani, E.; Battistini, L.; Zanardi, F.; Curti, C.; Nicastro, G.; Belvisi, L.; Motto, I.; Castorina, M.; Giannini, G.; Pisano, C. Grafting aminocyclopentane carboxylic acids onto the RGD tripeptide sequence generates low nanomolar $\alpha_V\beta_3/\alpha_V\beta_5$ integrin dual binders. *J. Med. Chem.* **2005**, *48*, 7675–7687. (h) Marugán, J. J.; Manthey, C.; Anaclerio, B.; Lafrance, L.; Lu, T.; Markotan, T.; Leonard, K. A.; Crysler, C.; Eisennagel, S.; Dasgupta, M.; Tomczuk, B. Design, synthesis, and biological evaluation of novel potent and selective $\alpha_V\beta_3/\alpha_V\beta_5$ integrin dual inhibitors with improved bioavailability. Selection of the molecular core. *J. Med. Chem.* **2005**, *48*, 926–934. (i) Salvati, M.; Cordero, F. M.; Pisaneschi, F.; Cini, N.; Bottoncetti, A.; Brandi, A. New cyclic Arg-Gly-Asp pseudopentapeptide containing the β-turn mimetic GPTM. *Synlett* **2006**, 2067–2070. (j) Urman, S.; Gaus, K.; Yang, Y.; Strijowski, V.; Sewald, N.; De Pol, S.; Reiser, O. The constrained amino acid β-Acc confers potency and selectivity to integrin ligands. *Angew. Chem., Int. Ed.* **2007**, *46*, 3976–3978. (k) Gentilucci, L.; Cardillo, G.; Squassabia, F.; Tolomelli, A.; Spampinato, S.; Sparta, A.; Baiula, M. Inhibition of cancer cell adhesion by heterochiral Pro-containing RGD mimetics. *Bioorg. Med. Chem. Lett.* **2007**, *17*, 2329–2333. (l) Dijkgraaf, I.; Rijnders, A. Y.; Soede, A.; Dechesne, A. C.; van Esse, G. W.; Brouwer, A. J.; Corstens, F. H. M.; Boerman, O. C.; Rijkers, D. T. S.; Liskamp, R. M. Synthesis of DOTA-conjugated multivalent cyclic-RGD peptide dendrimers via 1,3-dipolar cycloaddition and their biological evaluation: implications for tumor targeting and tumor imaging purposes. *Org. Biomol. Chem.* **2007**, *5*, 935–944. (m) Heckmann, D.; Meyer, A.; Marinelli, L.; Zahn, G.; Stragies, R.; Kessler, H. Probing integrin selectivity: rational design of highly active and selective ligands for the $\alpha_5\beta_1$ and $\alpha_V\beta_3$ integrin receptor. *Angew. Chem., Int. Ed.* **2007**, *46*, 3571–3574. (n) Goodman, S. L.; Hölzemann, G.; Sulyok, G. A. G.; Kessler, H. Nanomolar small molecule inhibitors for $\alpha_V\beta_6$, $\alpha_V\beta_5$, and $\alpha_V\beta_3$ integrins. *J. Med. Chem.* **2002**, *45*, 1045–1051.

(8) For a recent report on the advanced clinical trials of compound **1**, see Stupp, R.; Rüegg, C. Integrin inhibitors reaching the clinic. *J. Clin. Oncol.* **2007**, *25*, 1637–1638.

(9) (a) Belvisi, L.; Riccioni, T.; Marcellini, M.; Vesci, L.; Chiarucci, I.; Efrati, D.; Potenza, D.; Scolastico, C.; Manzoni, L.; Lombardo, K.; Stasi, M. A.; Orlandi, A.; Ciucci, A.; Nico, B.; Ribatti, D.; Giannini, G.; Presta, M.; Carminati, P.; Pisano, C. Biological and molecular properties of a new $\alpha_V\beta_3/\alpha_V\beta_5$ integrin antagonist. *Mol. Cancer Ther.* **2005**, *4*, 1670–1680. (b) Belvisi, L.; Bernardi, A.; Colombo, M.; Manzoni, L.; Potenza, D.; Scolastico, C.; Giannini, G.; Marcellini, M.; Riccioni, T.; Castorina, M.; LoGiudice, P.; Pisano, C. Targeting integrins: insights into structure and activity of cyclic RGD pentapeptide mimics containing azabicycloalkane amino acids. *Bioorg. Med. Chem.* **2006**, *14*, 169–180.

(10) For a recent example of 14-membered RGD-based cyclic integrin binders, see ref 7i.

(11) For the role of proline and its substituted variants as privileged scaffolds in the synthesis of designed peptide and related molecules see, for example:(a) Ramesh, I.; Babu, I.; Ganesh, K. N. Enhanced triple helix stability of collagen peptides with 4*R*-aminoprolyl (Amp) residues: Relative roles of electrostatic and hydrogen bonding effects. *J. Am. Chem. Soc.* **2001**, *123*, 2079–2080. (b) Farrera-Sinfreu, J.; Zaccaro, L.; Vidal, D.; Salvatella, X.; Giralt, E.; Pons, M.; Albericio, F.; Royo, M. A new clas of foldamers based on *cis*-γ-amino-L-proline. *J. Am. Chem. Soc.* **2004**, *126*, 6048–6057. (c) Tamamura, H.; Araki, T.; Ueda, S.; Wang, Z.; Oishi, S.; Esaka, A.; Trent, J. O.; Nakashima, H.; Yamamoto, N.; Peiper, S. C.; Otaka, A.; Fujii, N. Identification of novel low molecular weight CXCR4 antagonists by structural tuning of cyclic tetrapeptide scaffolds. *J. Med. Chem.* **2005**, *48*, 3280–3289. (d) Gupta, S.; Macala, M.; Schafmeister, E. Synthesis of structurally diverse bis-peptide oligomers. *J. Org. Chem.* **2006**, *71*, 8691–8695. (e) Stragies, R.; Osterkamp, F.; Zischinsky, G.; Vossmeyer, D.; Kalkhof, H.; Reimer, U.; Zahn, G. Design and synthesis of a new class of selective integrin $\alpha_5\beta_1$ antagonists. *J. Med. Chem.* **2007**, *50*, 3786–3794.

(12) (a) For the use of integrin binder-bioactive moiety conjugates for therapeutical and diagnostic purposes see, for example Hynes, R. O. A reevaluation of integrins as regulators of angiogenesis. *Nat. Med.* **2002**, *8*, 918–921. (b) Janssen, M. L.; Oyen, W. J.; Dijkgraaf, I.; Massuger, L. F.; Frienlink, C.; Edwards, D. S.; Rajopadhye, M.; Boonstra, H.; Corstens, F. H.; Boerman, O. C. Tumor targeting with radiolabeled $\alpha_V\beta_3$ integrin binding peptides in a nude mouse model.

Cancer Res. **2002**, *62*, 6146–6151. (c) Nasongkla, N.; Shuai, X.; Ai, H.; Weinberg, B. D.; Pink, J.; Boothman, D. A.; Gao, J. cRGD-functionalized polymer micelles for targeted doxorubicin delivery. *Angew. Chem., Int. Ed.* **2004**, *43*, 6323–6327. (d) Chen, X.; Plencia, C.; Hou, Y.; Neamati, N. Synthesis and biological evaluation of dimeric RGD peptide-paclitaxel conjugate as a model for integrin-targeted drug delivery. *J. Med. Chem.* **2005**, *48*, 1098–1106 (corigendum, *J. Med. Chem.* **2005**, *48*, 5874). (e) Achilefu, S.; Bloch, S.; Markiewicz, M. A.; Zhong, T.; Ye, Y.; Dorshow, R. B.; Chance, B.; Liang, K. Synergistic effects of light-emitting probes and peptides for targeting and monitoring integrin expression. *Proc. Natl. Acad. Sci. U.S.A.* **2005**, *102*, 7976–7981. (f) Garanger, E.; Boturyn, D.; Jin, Z.; Dumy, P.; Favrot, M.-C.; Coll, J.-L. New multifunctional molecular conjugate vector for targeting, imaging, and therapy of tumors. *Mol. Ther.* **2005**, *12*, 1168–1175.

(13) Naturally occurring *trans*-4-hydroxy-L-proline is a inexpensive, enantiomerically pure starting material that can be bought from, for example, Sigma Aldrich at € 225,50 per 100 g (2007–2008 catalog, € 0,30 per mmol).

(14) *cis*-4-Hydroxy-D-proline (**14**) is commercially available, but it can be conveniently obtained from its renowned relative **13** by facile epimerization at C2 (see ref 1 in the Supporting Information).

(15) Calvete, J. J. Structure-function correlations of snake venom disintegrin. *Curr. Pharm. Des.* **2005**, *11*, 829–835.

(16) Belkin, V. M.; Belkin, A. M.; Koteliansky, V. E. Human smooth muscle VLA-1 integrin: purification, substrate specificity, localization in aorta, and expression during development. *J. Cell Biol.* **1990**, *111*, 2159–2170.

(17) Pytela, R.; Pierschbacher, M. D.; Argraves, S.; Suzuki, S.; Ruoslahti, E. Arginine-glycine-aspartic acid adhesion receptors. *Methods Enzymol.* **1987**, *144*, 475–489.

(18) (a) Kumar, C. C.; Nie, H.; Rogers, C. P.; Malkowski, M.; Maxwell, E.; Catino, J. J.; Armstrong, L. Biochemical characterization of the binding of echistatin to integrin $\alpha_V\beta_3$ receptor. *J. Pharmacol. Exp. Ther.* **1997**, *283*, 843–853. (b) Kumar, C. C.; Malkowski, M.; Yin, Z.; Tanghetti, E.; Yaremko, B.; Nechuta, T.; Varner, J.; Liu, M.; Smith, E. M.; Neustadt, B.; Presta, M.; Armstrong, L. Inhibition of angiogenesis and tumor growth by SCH221153, a dual $\alpha_V\beta_3$ and $\alpha_V\beta_5$ integrin receptor antagonist. *Cancer Res.* **2001**, *61*, 2232–2238.

(19) (a) The occurrence of two (or multiple) ligand-bound states for certain receptors has been widely reported. See, for example: Clark, E. A.; Hill, S. J. Differential effect of sodium ions and guanine nucleotides on the binding of thioperamide and clobenpropit to histamine H_3-receptors in rat cerebral cortical membranes. *Br. J. Pharmacol.* **1995**, *114*, 357–362. (b) Bellier, B.; McCort-Tranchepain, I.; Ducos, B.; Danascimento, S.; Meudal, H.; Noble, F.; Garbay, C.; Roques, B. P. Synthesis and biological properties of new constrained CCK-B antagonists: discrimination of two affinity states of the CCK-B receptor on transfected CHO cells. *J. Med. Chem.* **1997**, *40*, 3947–3956.

(20) (a) Bednar, R. A.; Gaul, S. L.; Hamill, T. G.; Egbertson, M. S.; Shafer, J. A.; Hartman, G. D.; Gould, R. J.; Bednar, B. Identification of low molecular weight GPIIb/IIIa antagonists that bind preferentially to activated platelets. *J. Pharmacol. Exp. Ther.* **1998**, *285*, 1317–1326. (b) Egbertson, M. S.; Cook, J. J.; Bednar, B.; Prugh, J. D.; Bednar, R. A.; Gaul, S. L.; Gould, R. J.; Hartman, G. D.; Homnick, C. F.; Holahan, M. A.; Libby, L. A.; Lynch, J. J.; Lynch, R. J.; Sitko, G. R.; Stranieri, M. T.; Vassallo, L. M. Non-peptide GPIIb/IIIa inhibitors. 20. Centrally constrained thienothiophene α-sulfonamides are potent, long acting in vivo inhibitors of platelet aggregation. *J. Med. Chem.* **1999**, *42*, 2409–2421. (c) García, A. J.; Schwarzbauer, J. E.; Boettiger, D. Distinct activation states of $\alpha_5\beta_1$ integrin show differential binding to RGD and synergy domains of fibronectin. *Biochemistry* **2002**, *41*, 9063–9069.

(21) (a) Takagi, J.; Petre, B. M.; Walz, T.; Springer, T. A. Global conformational rearrangements in integrin extracellular domains in outside-in and inside-out signaling. *Cell* **2002**, *110*, 599–611. (b) Shimaoka, M.; Springer, T. A. Therapeutic antagonists and conformational regulation of integrin function. *Nat. Rev. Drug Discovery* **2003**, *2*, 703–716. (c) Humphries, M. J.; McEwan, P. A.; Barton, S. J.; Buckley, P. A.; Bella, J.; Mould, A. P. Integrin structure: Heady advances in ligand binding, but activation still makes the knees wobble. *Trends Biochem. Sci.* **2003**, *28*, 313–320. (d) Xiao, T.; Takagi, J.; Coller, B. S.; Wang, J.-H.; Springer, T. A. Structural basis for allostery in integrins and binding to fibrinogen-mimetic therapeutics. *Nature* **2004**, *432*, 59–67.

(22) (a) Xiong, J.-P.; Stehle, T.; Diefenbach, B.; Zhang, R.; Dunker, R.; Scott, D. L.; Joachimiak, A.; Goodman, S. L.; Arnaout, M. A. Crystal structure of the extracellular segment of integrin $\alpha_V\beta_3$. *Science* **2001**, *294*, 339–345. (b) Xiong, J. P.; Stehle, T.; Zhang, R.; Joachimiak, A.; Frech, M.; Goodman, S. L.; Arnaout, M. A. Crystal structure of the extracellular segment of integrin $\alpha_V\beta_3$ in complex with an Arg-Gly-Asp ligand. *Science* **2002**, *296*, 151–155.

(23) (a) It has been demonstrated that certain macromolecular ligands (e.g., echistatin, fibronectin, monoclonal antibodies), in addition to the pivotal RGD-recognition motif, utilize auxiliary binding determinants for selective interaction with two distinct sites within the integrin receptor. See, for example Wierzbicka-Patynowski, I.; Niewiarowski, S.; Marcinkiewicz, C.; Calvete, J. J.; Marcinkiewicz, M. M.; McLane, M. A. Structural requirements of echistatin for the recognition of $\alpha_V\beta_3$ and $\alpha_5\beta_1$ integrins. *J. Biol. Chem.* **1999**, *274*, 37809–37814. (b) Yahalom, D.; Wittelsberger, A.; Mierke, D. F.; Rosenblatt, M.; Alexander, J. M.; Chorev, M. Identification of the principal binding site for RGD-containing ligands in the $\alpha_V\beta_3$ integrin: A photoaffinity cross-linking study. *Biochemistry* **2002**, *41*, 8321–8331. (c) DelGatto, A.; Zaccaro, L.; Grieco, P.; Novellino, E.; Zannetti, A.; Del Vecchio, S.; Iommelli, F.; Salvatore, M.; Pedone, C.; Saviano, M. Novel and selective $\alpha_V\beta_3$ receptor peptide antagonist: Design, synthesis, and biological behavior. *J. Med. Chem.* **2006**, *49*, 3416–3420, see also refs 20c and 21d.

(24) The use of the mean IC_{50} for an initial SAR evaluation has already been adopted by several authors. Nonetheless, with the possibility in sight of using these integrin binders as antagonists for in vivo intervention, the IC_{50h} values ought to portray a more realistic estimate of their efficacy as ligands. For a discussion on these themes see, for example, refs 19b and 20a.

(25) For the calculation of the averaged binding affinity, we used the following equation: $IC_{50} = IC_{50l} \times 10\exp[(\%_h/100) \times \mathrm{Log}(IC_{50h}/IC_{50l})]$, with IC_{50} values expressed in nM.

(26) (a) Rose, G. D.; Gierasch, L. M.; Smith, J. A. Turn in peptides and proteins. *Adv. Protein Chem.* **1985**, *37*, 1–109. (b) Guruprasad, K.; Prasad, M. S.; Kumar, G. R. Analysis of $\gamma\beta$, $\beta\gamma$, $\gamma\gamma$, $\beta\beta$ multiple turns in proteins. *J. Pept. Res.* **2000**, *56*, 250–263.

(27) A possible explanation for the obtained selectivity is that the integrin $\alpha_V\beta_5$-RGD binding site differs slightly in its β-region with respect to $\alpha_V\beta_3$ (the so-called specificity determining loop), making it less accommodating towards unsubstituted or substituted nitrogen atoms within the Amp-based ligands. For a comparative study on ligand selectivity toward the $\alpha_V\beta_3$ and $\alpha_V\beta_5$ integrin subtypes, see: Marinelli, L.; Gottschalk, K.-E.; Meyer, A.; Novellino, E.; Kessler, H. Human integrin $\alpha_V\beta_5$: Homology modelling and ligand binding. *J. Med. Chem.* **2004**, *47*, 4166–4177.

(28) Morris, G. M.; Goodsell, D. S.; Halliday, R. S.; Huey, R.; Hart, W. E.; Belew, R. K.; Olson, A. J. Automated docking using a Lamarckian genetic algorithm and an empirical binding free energy. *J. Comput. Chem.* **1998**, *19*, 1639–1662.

(29) For readers convenience, a schematic, bidimensional view of observed interactions between picomolar ligand **9** and the protein (Figure S17), as well as surface representations of the $\alpha_V\beta_3$ ligand-binding site with compounds **5**, **9**, and **10** (Figure S18) are reported in the Supporting Information.

(30) (a) Csermely, P.; Agoston, V.; Pongor, S. The efficiency of multi-target drugs: The network approach might help drug design. *Trends Pharmacol. Sci.* **2005**, *26*, 178–182. (b) Espinoza-Fonseca, L. M. The benefits of the multi-target approach in drug design and discovery. *Bioorg. Med. Chem.* **2006**, *14*, 896–897. (c) Hopkins, A. L.; Mason, J. S.; Overington, J. P. Can we rationally design promiscuous drugs. *Curr. Opin. Struct. Biol.* **2006**, *16*, 127–136. (d) DeNardo, S. J. Combined molecular targeting for cancer therapy: A new paradigm in need of molecular imaging. *J. Nucl. Med.* **2006**, *47*, 4–5.

(31) Kuphal, S.; Bauer, R.; Bosserhoff, A.-K. Integrin signalling in malignant melanoma. *Cancer Metastasis Rev.* **2005**, *24*, 195–222.

(32) Kumar, C. C.; Nie, H.; Armstrong, L.; Zhang, R.; Vijay-Kumar, S.; Tsarbopoulos, A. Chloramine T-induced structural and biochemical changes in echistatin. *FEBS Lett.* **1998**, *429*, 239–248.

(33) Orlando, R. A.; Cheresh, D. A. Arginine-glycine-aspartic acid binding leading to molecular stabilization between integrin $\alpha_V\beta_3$ and its ligand. *J. Biol. Chem.* **1991**, *266*, 19543–19550.

(34) States, D. J.; Haberkorn, R. A.; Ruben, D. J. A two-dimensional nuclear Overhauser experiment with pure absorption phase in four quadrants. *J. Magn. Reson.* **1982**, *48*, 286–292.

(35) Wüthrich, K. *NMR of Proteins and Nucleic Acids*; John Wiley & Sons: New York, 1986.

(36) Gillet, A; Sanner, M.; Stoffler, D.; Olson, A. Tangible interfaces for structural molecular biology. *Structure* **2005**, *13*, 483–491.

JM701214Z